This article has been accepted for publication in a future issue of this journal, but has not been fully edited. Content may change prior to final publication. Citation information: DOI 10.1109/ACCESS.2018.2859794, IEEE Access

Transmit Antenna Combination Optimization for Generalized Spatial Modulation Systems

Lixia Xiao, Pei Xiao, *Senior Member, IEEE*, Yue Xiao, *Member, IEEE*, Chaowu Wu, Hung Viet Nguyen *Member, IEEE*, Ibrahim Hemadeh, and Lajos Hanzo, *Fellow, IEEE*

***Abstract*—Generalized Spatial Modulation (GSM), where both the Transmit Antenna Combination (TAC) index and the Amplitude Phase Modulation (APM) symbols convey information, is a novel low-complexity and high efficiency Multiple Input Multiple Output (MIMO) technique. In Conventional GSM (C-GSM), the legitimate TACs are selected randomly to transmit the APM symbols. However, the number of the TACs must be a power of two, hence the excess TACs are discarded, resulting in wasting some resource. To address these issues, in this paper, an optimal TAC set-aided Enhanced GSM (E-GSM) scheme is proposed, where the optimal TAC set is selected with the aid of the Channel State Information (CSI) by maximizing the Minimum Euclidean Distance (MED). Furthermore, a Hybrid Mapping GSM (HM-GSM) scheme operating without CSI knowledge is investigated, where the TAC selection and bit-to-TAC mapping are both taken into consideration for optimizing the Average Hamming Distance (AHD). Finally, an Enhanced High Throughput GSM (E-HT-GSM) scheme is developed, which makes full use of all the TACs. This scheme is capable of achieving an extra one bit transmission rate per time slot. Moreover, rotated phase is employed and optimized for the reused TACs. Our simulation results show that the proposed E-GSM system and HM-GSM system are capable of outperforming the C-GSM system. Furthermore, the E-HT-GSM system is capable of obtaining one extra bit transmission rate per time slot compared to the C-GSM system.**

***Index Terms*—Generalized Spatial Modulation (GSM), Transmit Antennas Combination (TACs), Average Hamming Distance (AHD).**

List of Acronyms

ABEP	Average Bit Error Probability
AMP	Amplitude Phase Modulation
AHD	Average Hamming Distance
BER	Bit Error Rate
C-GSM	Conventional Generalized Spatial Modulation
CS	Compressive Sensing
CSI	Channel State Information
ED	Euclidean Distances
E-GSM	Enhanced Generalized Spatial Modulation
E-HT-GSM	Enhanced High Throughput GSM
GSM	Generalized Spatial Modulation
HD	Hamming Distance
HM-GSM	Hybrid Mapping based GSM
ML	Maximum Likelihood
MED	Minimum Euclidean Distance
MIMO	Multiple Input Multiple Output
PEP	Pairwise Error Probability
RF	Radio Frequency
SM	Spatial Modulation
TA	Transmit Antennas
TAC	Transmit Antenna Combination

L. Xiao, P. Xiao, Ibrahim Hemadeh and H. V. Nguyen are with the school of Electrical Electronic Engineering of University of Surrey.

Y. Xiao and C. Wu are with the National Key Laboratory of Science and Technology on Communications, University of Electronic Science and Technology of China 611731, Sichuan, China.

L. Hanzo is with the school of Electronics and Computer Science, University of Southampton, Southampton SO17 1BJ, U.K. (email: lh@ecs.soton.ac.uk).

L. Hanzo would also like to thank the ERC for the financial support of this Advanced Fellow grants.

List of Symbols

B	Transmission rate
B_1	The number of bits that one TAC index carried
B_2	The number of bits that APM symbols carried
$C_{N_t}^{N_u}$	The total number of TACs
$C_{\text{C-GSM}}$	The complexity of C-GSM system
$C_{\text{E-GSM}}^{\text{Op}}$	The complexity of optimal TAC selection
$D(\bar{\varsigma})$	The value of AHD
$F(\bar{\varsigma})$	The value of PEP
$\mathbf{H}$	The channel matrix
$\mathbb{I}_q$	The q-th TAC set
$\mathbb{I}_{\text{all}}$	The TAC set including all the TACs
I_j	The j-th TAC
M	The modulation order of APM
N_t	The total number of TAs
N_u	The number of activated TAs
N_{all}	The total number of TACs
N	The number of one legitimate TAc set
N_{left}	The number of discarded TACs
N_r	The number of receiver antennas
$\mathbf{n}$	The noise matrix
P_b	The ABEP of GSM system
$\mathbf{y}$	The receive signal

I. Introduction

GENERALIZED Spatial Modulation (GSM) [1]-[2] is a novel low-complexity high-efficiency scheme relying on a reduced number of Radio Frequency (RF) chain

This work is licensed under a Creative Commons Attribution 3.0 License. For more information, see http://creativecommons.org/licenses/by/3.0/.

This article has been accepted for publication in a future issue of this journal, but has not been fully edited. Content may change prior to final publication. Citation information: DOI 10.1109/ACCESS.2018.2859794, IEEE Access

for Multi-Input Multi-Output (MIMO) transmission. In the GSM scheme, multiple Transmit Antennas (TAs) are activated symbol in each interal, hence GSM may be flexibly reconfigured between Spatial Modulation (SM) [3]-[5] and Spatial Multiplexing [6]. Specifically, in the GSM scheme, the information bits are conveyed by the index of the activated Transmit Antenna Combination (TAC) as well as by the Amplitude Phase Modulation (APM) symbols. Consequently, the GSM scheme attains a high bandwidth efficiency, despite using a low number of RF chains at the transmitter. Several independent studies have proved that SM and GSM are both promising candidates in the future wireless communications [7]-[11].

In GSM systems, N_u out of N_t ($N_u < N_t$) TAs are activated for data transmission, so that $N_{\text{all}} = C_{N_t}^{N_u}$ legitimate TACs are available. Among them, $N = 2^{\lfloor \log_2(C_{N_t}^{N_u}) \rfloor}$ TACs are chosen randomly for encoding the information bits, where $\lfloor \bullet \rfloor$ denotes the floor operation and C_x^y represents the binary coefficient. The remaining $N_{\text{left}} = (N_{\text{all}} - N)$ TACs are discarded, hence resulting in wasting some resource. Therefore, how to choose the optimal TAC set and exploiting the remaining TACs become challenging research problems.

Early contributions on GSM have been mainly focused on the low-complexity receiver design [12]-[19], on the performance and achieve rate analysis [20]-[22], and on their applications for specific communication scenarios [23]. Specifically, the authors of [12] proposed a low-complexity near- Maximum Likelihood (ML) detector. The detectors of [13]-[16] exhibited a considerably reduced complexity, since the sparsity of the activated antennas was exploited based on the classic Compressive Sensing (CS) algorithms. The threshold-aided CS detector of [16] is capable of striking a better trade-off between the performance and complexity than other detection schemes. Moreover, the detector of [17] employed both forward error correction codes and turbo equalization to achieve the highest possible coding gain. Additionally, the low-complexity GSM conceived receiver design for dispersive channels have been investigated in [18] and [19]. On the other hand, the capacity of GSM system was analyzed in [20]-[22] and the achievable rate was quantified in [21]. Since its high capacity and energy efficiency, GSM is a promising candidate for millimeter-wave communications [23]. However, the above research did not consider the Channel Sate Information (CSI) at the transmitter.

Recently, some transceiver designs of SM-based systems were developed in [24]-[32], as shown in Table I. Moreover, the CSI based link adaptation, antenna selection-aided distributed/cooperative protocols and precoding were investigated in [33]-[40] for SM, as shown in Table II. However, to the best of our knowledge how to select the TAC of GSM has not been investigated to date. Against the above background, the major contributions of this paper are summarized as follows:

1) An Enhanced GSM (E-GSM) system is proposed, where the TAC set is selected by exploiting the knowledge of the CSI based on maximizing the Minimum Euclidean Distance (MED). A low-complexity optimal TAC selection algorithm is developed for the E-GSM system. Our simulation results show that the proposed E-GSM scheme is capable of providing considerable performance gain over the Conventional GSM (C-GSM) system.
2) A Hybrid Mapping based GSM (HM-GSM) system operating without CSI knowledge is developed, where the TAC selection and bit-to-TAC mapping are both taken into consideration for improving the Average Bit Error Probability (ABEP).
3) Then an Enhanced Throughput GSM (E-HT-GSM) system is proposed, which conveys an extra bit. Specifically, the proposed E-HT-GSM system makes full use of all the TACs.

The remainder of this paper is organized as follows. Section II gives a rudimentary introduction of the C-GSM system. In Section III, the optimal-TAC-set based E-GSM with CSI is introduced and a low-complexity TAC selection algorithm is proposed. In Section IV, a hybrid bit-to-TAC mapping method dispensing with CSI knowledge is proposed for the HM-GSM system to achieve a better ABEP. In Section V, an E-HT-GSM scheme is proposed, where all the TACs are exploited and the phase optimization as well as its performance analysis is offered in Section V. Section VI presents the simulation results, while Section VI concludes this paper. For reader's convenience, the full table of contents is include here.

Notation: $\|\cdot\|_F$ denotes the Frobenious norm of a matrix; $|\cdot|$ represents the magnitude of a complex quantity; $(\cdot)^T$ and $(\cdot)^H$ stand for the transpose and the Hermitian transpose of a vector/matrix, respectively.

II. Conventional GSM

In C-GSM systems, N_u out of N_t ($N_u < N_t$) TAs are activated for data transmission, so that $C_{N_t}^{N_u}$ legitimate TACs are available, and $N = 2^{\lfloor \log_2(C_{N_t}^{N_u}) \rfloor}$ TACs are exploited for encoding the information bits. In each time slot, a vector of B information bits is partitioned in two parts, where $B_1 = \lfloor \log_2(C_{N_t}^{N_u}) \rfloor$ bits are used to select a TAC I_i ($i \in (1, N)$), and $B_2 = N_u \log_2(M)$ bits are used to modulate N_u M-APM symbols. Hence, the C-GSM transmit vector can be represented as

$$\mathbf{x}_{(I_i,\mathbf{s})} = \left[..., 0, s_{i_1}, 0, ..., 0, s_{i_2}, 0..., 0, s_{i_{N_u}}, 0, ... \right]^T, \quad (1)$$

where $(i_1, ..., i_{N_u})$ indicates the activated TA indices.

Let $\mathbf{H} \in \mathbb{C}^{N_r \times N_t}$ and $\mathbf{n} \in \mathbb{C}^{N_r \times 1}$ be the MIMO channel matrix and noise matrix, whose entries are complex-valued Gaussian distributed, yielding $\mathcal{CN}(0,1)$ and $\mathcal{CN}(0,\sigma^2)$, respectively. The received signal $\mathbf{y} \in \mathbb{C}^{N_r \times 1}$ can be formulated as

$$\mathbf{y} = \mathbf{H}\mathbf{x}_{(I_i,\mathbf{s}_i)} + \mathbf{n} = \sum_{t=i_1}^{i_{N_u}} \mathbf{h}_t s_t + \mathbf{n} = \mathbf{H}_{I_i}\mathbf{s}_i + \mathbf{n}, \quad (2)$$

where $\mathbf{H}_{I_i} = (\mathbf{h}_{i_1}, \mathbf{h}_{i_2}, ..., \mathbf{h}_{i_{N_u}})$ is the sub-matrix of $\mathbf{H}$ with N_u columns, and $\mathbf{s}_i = (s_{i_1}, ..., s_{i_{N_u}})^T$ is the transmit symbol vector corresponding to the TAC $I_i = (i_1, ..., i_{N_u})$.

This work is licensed under a Creative Commons Attribution 3.0 License. For more information, see http://creativecommons.org/licenses/by/3.0/.

This article has been accepted for publication in a future issue of this journal, but has not been fully edited. Content may change prior to final publication. Citation information: DOI 10.1109/ACCESS.2018.2859794, IEEE Access

It follows from Eq. (2) that, the optimal ML-based demodulator can be formulated as

$$(\hat{I}, \hat{\mathbf{s}})_{\mathrm{ML}} = \arg\min_{I \in \mathbb{I}, \mathbf{s} \in \mathbb{S}} \|\mathbf{y} - \mathbf{H}_I \mathbf{s}\|_F^2 \,, \tag{3}$$

where $\mathbb{I} = [I_1, I_2, ..., I_N]$ is the set of TAC, and $\mathbb{S}$ is the set of N_u-element symbol vector.

III. Transmit antenna combination selection for the GSM System relying on channel state information

In the C-GSM system, N legitimate TACs are selected randomly from $C_{N_t}^{N_u}$ ones, whose performance can be further improved by selecting the optimal TAC set. In this section, an optimal TAC set based E-GSM system is proposed, where N legitimate TACs are obtained utilizing the CSI instead of selecting them randomly based on maximizing the MED of GSM system. Then, a low-complexity optimal algorithm is introduced.

A. Optimal TAC Set Based E-GSM

For the C-GSM system having N_t TAs and N_u activated TAs, there are a total of $N_{\mathrm{all}} = C_{N_t}^{N_u}$ TACs, and N out of N_{all} TACs are selected randomly. Hence, there are $C_{N_{\mathrm{all}}}^{N}$ possible TAC sets $\mathbb{I}_q$, $q = (1, ..., C_{N_{\mathrm{all}}}^{N})$. In the C-GSM system, a specific TAC set is selected randomly from $\{\mathbb{I}_1, ..., \mathbb{I}_{C_{N_{\mathrm{all}}}^{N}}\}$. In this section, the optimal TAC set having the largest MED is selected from the $C_{N_{\mathrm{all}}}^{N}$ TAC sets, as shown in Fig. 1. More specifically, for each TAC set $\mathbb{I}_q$, the MED of the specific channel matrix $\mathbf{H}$ between the two GSM symbols $\mathbf{x}_m$ and $\mathbf{x}_n$ can be defined as [31]

$$\begin{aligned} d_{\min}^q &= \min_{\mathbf{x}_m \neq \mathbf{x}_n} ||\mathbf{H}\mathbf{x}_m - \mathbf{H}\mathbf{x}_n||_F^2 \\ &= \min_{I_m, I_n \in \mathbb{I}_q, (I_m, \mathbf{s}_m) \neq (I_n, \mathbf{s}_n)} ||\mathbf{H}_{I_m}\mathbf{s}_m - \mathbf{H}_{I_n}\mathbf{s}_n||_F^2 . \end{aligned} \tag{4}$$

where $I_m = (m_1, m_2, ..., m_{N_u})$ and $I_n = (n_1, n_2, ..., n_{N_u})$ denote two TACs. For $C_{N_{\mathrm{all}}}^{N}$ TAC sets we have $C_{N_{\mathrm{all}}}^{N}$ MEDs and the optimal TAC set index having the largest MED can be obtained as

$$\hat{q} = \arg \max_{q \in \{1, 2, ..., C_{N_{\mathrm{all}}}^{N}\}} (d_{\min}^q). \tag{5}$$

Then the optimal TAC set for the specific channel matrix is $\mathbb{I}_{\hat{q}}$. In the optimal TAC set selection, we have to calculate $C_{N_{\mathrm{all}}}^{N}$ MEDs. For each MED, NM^{N_u} Euclidean distances have to be calculated to get the minimum one. Hence, a total of $C_{N_{\mathrm{all}}}^{N} NM^{N_u}$ Euclidean Distances (ED) should be computed for the optimal TAC set section. In fact, there are too many MEDs that are repeatly calculated. Hence, the optimal TAC set selection can be simplified by computing each ED only once. Assuming that the set $\mathbb{I}_{\mathrm{all}}$ contains all the TACs as $\mathbb{I}_{\mathrm{all}} = [I_1, ..., I_N, ..., I_{N_{\mathrm{all}}}]$, each TAC corresponding to M^{N_u} GSM symbols, the set $\mathbb{X}_{\mathrm{all}}$ containing $N_{\mathrm{all}} M^{N_u}$ possible GSM vectors is expressed as

$$\mathbb{X}_{\mathrm{all}} = [\mathbf{x}_1, ..., \mathbf{x}_{NM^{N_u}}, ..., \mathbf{x}_{N_{\mathrm{all}} M^{N_u}}], \tag{6}$$

Then, the ED of a specific channel matrix $\mathbf{H}$ between the two different GSM symbols $\mathbf{x}_m \in \mathbb{X}_{\mathrm{all}}$ and $\mathbf{x}_n \in \mathbb{X}_{\mathrm{all}}$ can be defined as

$$d_{m,n} = ||\mathbf{H}\mathbf{x}_m - \mathbf{H}\mathbf{x}_n||_F^2, m \neq n. \tag{7}$$

There are a total of $(N_{\mathrm{all}} M^{N_u} - 1)^2$ $\{d_{m,n}\}_{m \neq n = 1}^{N_{\mathrm{all}} M^{N_u}}$ values and we only have to calculate $(N_{\mathrm{all}} M^{N_u} - 1)^2/2$ values due to the symmetry of the GSM symbols ($d_{m,n} = d_{n,m}$). The simplified optimal TAC set selection works follows.

Step 1: Obtain the $(N_{\mathrm{all}} M^{N_u} - 1)^2$ values of $d_{m,n}$ according to (7), which is shown in Table III, where we have $N_M = M^{N_u}$ and $d_{m,n} = d_{n,m}$.

Step 2: Obtain the legitimate TAC sets $\mathbb{I}_q$, $q = (1, ..., C_{N_{\mathrm{all}}}^{N})$.

Step 3: For each TAC set $\mathbb{I}_q$, find the $d_{\min}^q$ based on Table III. Specifically, if we have $\mathbb{I}_q = [I_1, ..., I_N]$, we find the MED $d_{\min}^q$ from the values of $d_{m,n}$ corresponding to $\mathbb{I}_q$ based on Table III.

Step 4: Get the optimal TAC set index by (5).

Although the simplified optimal TAC set can be obtained by only calculating $(N_{\mathrm{all}} M^{N_u} - 1)^2/2$ EDs, its complexity is still excessive for large values of N_t and N_u. Next, a simplified optimal TAC set selection algorithm is introduced.

B. Low-Complexity Optimal TAC Selection Based E-GSM

In this section, low-complexity optimal TAC selection algorithms are developed for $M = 1$ and $M > 1$ respectively. Specifically, for the case of $M = 1$, the activated antenna indices transmit the symbol '1', which is also termed as Generalized Space Shift Keying (GSSK) scheme [41].

1) TAC Design for $M = 1$:

For the case of $M = 1$, the activated TAC transmits the symbol '1', so that the ED matrix can be defined as

$$\mathbf{W} = \begin{bmatrix} w_{11} & w_{12} & \cdots & w_{1N_{\mathrm{all}}} \\ w_{21} & w_{22} & \cdots & w_{2N_{\mathrm{all}}} \\ \vdots & \vdots & \ddots & \vdots \\ w_{N_{\mathrm{all}}1} & w_{N_{\mathrm{all}}2} & \cdots & w_{N_{\mathrm{all}}N_{\mathrm{all}}} \end{bmatrix}, \tag{8}$$

where the element w_{mn}, $m = (1, ..., N_{\mathrm{all}})$, $n = (1, ..., N_{\mathrm{all}})$ denotes the ED between two GSM symbols as

$$\begin{aligned} & w_{mn} = ||\mathbf{H}_{I_m} - \mathbf{H}_{I_n})||_F^2 \\ & = \left\|(\mathbf{h}_{m_1} + \mathbf{h}_{m_2} + \cdots \mathbf{h}_{m_{N_u}}) - (\mathbf{h}_{n_1} + \mathbf{h}_{n_2} + \cdots \mathbf{h}_{n_{N_u}})\right\|_F^2 \\ & = \begin{cases} 0, & \mathrm{if} I_m = I_n \\ ||\mathbf{H}_{D_m} - \mathbf{H}_{D_n})||_F^2, & \mathrm{if} I_m \neq I_n, \end{cases} \end{aligned} \tag{9}$$

where D_m and D_n represent the different elements between I_m and I_n. Assuming that the identical element set between I_m and I_n is $\Lambda = \mathrm{intersect}(I_m, I_n)$, the values of D_m and D_n are obtained by

$$D_m = \mathrm{setdiff}(I_m, \Lambda), D_n = \mathrm{setdiff}(I_n, \Lambda) \ , \tag{10}$$

where intersect(A, B) denotes the function returning the identical elements between A and B, while setdiff(A, B)

This work is licensed under a Creative Commons Attribution 3.0 License. For more information, see http://creativecommons.org/licenses/by/3.0/.

This article has been accepted for publication in a future issue of this journal, but has not been fully edited. Content may change prior to final publication. Citation information: DOI 10.1109/ACCESS.2018.2859794, IEEE Access

denotes the function returning different elements between A and B. As a result, (5) can be reformulated as

$$\begin{aligned} d^q_{\min} &= \min_{\mathbf{x}_m \neq \mathbf{x}_n} ||\mathbf{H}\mathbf{x}_m - \mathbf{H}\mathbf{x}_n||^2_F \\ &= \min_{\forall D_m, D_n} ||\mathbf{H}_{D_m} - \mathbf{H}_{D_n})||^2_F. \end{aligned} \tag{11}$$

For $q = (1, ..., C^N_{N_{\text{all}}})$, there are a lot of repeated calculations of $||\mathbf{H}_{D_m} - \mathbf{H}_{D_n})||^2_F$. To reduce the complexity of finding the optimal set based TAC selection, only the different values of $||\mathbf{H}_{D_m} - \mathbf{H}_{D_n})||^2_F$ are calculated.

For the generalized cases of $I_m = (m_1, m_2, ..., m_{N_u})$ and $I_n = (n_1, n_2, ..., n_{N_u})$, assuming that the size of Λ is β, the number of elements in D_m and D_n are $N_u - \beta$. Then the number of the identical values of $||\mathbf{H}_{D_m} - \mathbf{H}_{D_n})||^2_F$ is

$$N_{\text{same}} = 2(C^{\beta}_{N_t - 2(N_u - \beta)}). \tag{12}$$

As a result, the number of different nonzero values of $||\mathbf{H}_{D_m} - \mathbf{H}_{D_n})||^2_F$ in the ED matrix $\mathbf{W}$ is

$$N_{ED} = \sum_{\beta=0}^{N_u - 1} \frac{C^{\beta}_{N_t} C^{N_u-\beta}_{N_t-\beta} C^{N_u-\beta}_{N_t-\beta-N_u}}{2}. \tag{13}$$

For the generalized cases, there are a total of N_{all} TACs and $(N_{\text{all}} - N)$ TACs have to be removed from $\mathbb{I}_{\text{all}}$. After obtaining the N_{ED} different EDs $\mathbf{w} = [w_1, ..., w_{N_{ED}}]$, the TAC selection for $M = 1$ operates as follows.

Step 1: Obtain the ED matrix $\mathbf{W}$ based on N_{ED} different EDs $\mathbf{w} = [w_1, ..., w_{N_{ED}}]$.

Step 2: Sort the N_{ED} EDs in an ascending order as

$$[v_1, v_2, ...v_{N_{ED}}] = \text{sort}(\mathbf{w}, `ascend'). \tag{14}$$

Step 3: Remove all the values of v_1 v_2,..., in the sequence from the matrix $\mathbf{W}$ until we removed N_{left} TACs defining $\mathbb{I}_{\text{Re}}$.

Step 4: Obtain the optimal TAC set as $\mathbb{I}_o = \mathbb{I}_{\text{all}} \backslash \mathbb{I}_{\text{Re}}$.

Considering $N_t = 4$ $N_u = 2$ for example, the EDs between any two GSM symbols are presented in Table IV and we have

$$\begin{aligned} &w_{12} = w_{21} = w_{56} = w_{65} = ||\mathbf{h}_2 - \mathbf{h}_3||^2_F; \\ &w_{13} = w_{31} = w_{46} = w_{64} = ||\mathbf{h}_2 - \mathbf{h}_4||^2_F; \\ &w_{14} = w_{41} = w_{36} = w_{63} = ||\mathbf{h}_1 - \mathbf{h}_3||^2_F; \\ &w_{15} = w_{51} = w_{26} = w_{62} = ||\mathbf{h}_1 - \mathbf{h}_4||^2_F; \\ &w_{16} = w_{61} = ||(\mathbf{h}_1 + \mathbf{h}_2) - (\mathbf{h}_3 + \mathbf{h}_4)||^2_F; \\ &w_{23} = w_{32} = w_{45} = w_{54} = ||\mathbf{h}_3 - \mathbf{h}_4||^2_F; \\ &w_{24} = w_{42} = w_{35} = w_{53} = ||\mathbf{h}_1 - \mathbf{h}_2||^2_F; \\ &w_{25} = w_{52} = ||(\mathbf{h}_1 + \mathbf{h}_3) - (\mathbf{h}_2 + \mathbf{h}_4)||^2_F; \\ &w_{34} = w_{43} = ||(\mathbf{h}_1 + \mathbf{h}_4) - (\mathbf{h}_2 + \mathbf{h}_3)||^2_F. \end{aligned} \tag{15}$$

As a result, there are only a total of 9 EDs $\mathbf{w} = [w_{12}, w_{13}, w_{14}, w_{15}, w_{16}, w_{23}, w_{24}, w_{25}, w_{34}]$ to be computed for TAC selection. If the minimum value of $\mathbf{w}$ is w_{12}, the removed TAC set $\mathbb{I}_{\text{Re}}$ may represent any of the combinations $\{(I_1, I_5), (I_1, I_6), (I_2, I_5), (I_2, I_6)\}$.

2) TAC Design for $M > 1$:

For the case of $M > 1$, the elements in $\mathbf{W}$ of (8) can be defined as

$$\begin{aligned} w_{mn} &= \min_{\forall \mathbf{s}_m, \mathbf{s}_n} ||\mathbf{H}_{I_m}\mathbf{s}_m - \mathbf{H}_{I_n}\mathbf{s}_n||^2_F \\ &= \begin{cases} \min\limits_{\forall \mathbf{s}_m, \mathbf{s}_n} ||\mathbf{H}_{I_m}(\mathbf{s}_m - \mathbf{s}_n)||^2_F, \text{if} I_m = I_n, \mathbf{s}_m \neq \mathbf{s}_n \\ \min\limits_{\forall \mathbf{s}_m, \mathbf{s}_n} ||\mathbf{H}_{\Lambda}(\mathbf{s}^{\Lambda}_m - \mathbf{s}^{\Lambda}_n) + \mathbf{H}_{D_m}\bar{\mathbf{s}}^{\Lambda}_m - \mathbf{H}_{D_n}\bar{\mathbf{s}}^{\Lambda}_n||^2_F, \text{if} I_m \neq I_n \end{cases} \end{aligned} \tag{16}$$

where $\mathbf{s}^{\Lambda}_m$ and $\mathbf{s}^{\Lambda}_n$ represent the specific subsets of $\mathbf{s}_m$ and $\mathbf{s}_n$ corresponding to the Λ index set and $\bar{\mathbf{s}}^{\Lambda}_m = \mathbf{s}_m \backslash \mathbf{s}^{\Lambda}_m, \bar{\mathbf{s}}^{\Lambda}_n = \mathbf{s}_n \backslash \mathbf{s}^{\Lambda}_n$. Due to the associated symmetry, each w_{mn} can be obtained by computing $[(1 + M^{N_u})M^{N_u}]/2$ EDs in (16). Since we have $w_{mn} = w_{nm}$, the ED matrix $\mathbf{W}$ of (8) can be obtained by computing $N^M_{ED} = [(N_{all} + 1)N_{all}]/2$ different values w_{mn}. After obtaining the ED matrix $\mathbf{W}$, the TAC selection can be completed by the Steps.1-4 of the TAC design of $M = 1$.

Considering $N_t = 4$ $N_u = 2$ for example, the ED matrix $\mathbf{W}$ is presented in Table V, where w_{mn} can be obtained by computing 10 EDs. Observe from Eq. (15) and Tables IV-V that when the number of common minimum values of ED matrix $\mathbf{W}$ satisfied that $N_{\text{same}}/2 > N_{\text{left}}$, the minimum value will still exist after removing N_{left} TACs. In this case, the value of (11) is the same as that of the conventional TAC set.

C. Complexity Analysis of E-GSM Systems

In this section, the complexity orders of the ML-aided C-GSM and of the proposed E-GSM are compared in terms of the numbers of real-valued multiplications and additions. For the specific matrices of $\mathbf{A} \in \mathbb{C}^{m \times n}$, $\mathbf{B} \in \mathbb{C}^{n \times p}$, $\mathbf{c} \in \mathbb{C}^{n \times 1}$ and $\mathbf{d} \in \mathbb{C}^{n \times 1}$, the operations of $\mathbf{AB}$, $\|\mathbf{c}\|^2_F$ and $\mathbf{c} \pm \mathbf{d}$ require $8mnp - 2mp$, $4n - 1$, and $2n$ Floating-point operations (Flops), respectively. Accordingly, the complexity order of the C-GSM relying on the ML detector becomes

$$C_{\text{C-GSM}} = (8N_r N_u + 4N_r - 1)NM^{N_u}, \tag{17}$$

since the operation $||\mathbf{y} - \mathbf{H}_I\mathbf{s}||^2_F$ requires $C_F = (8N_r N_u + 4N_r - 1)$ Flops, and this operation is computed $2^B = NM^{N_u}$ times;

The complexity order of the low-complexity optimal TAC set based E-GSM system with ML detector is

$$C^{\text{Op}}_{\text{E-GSM}} = \begin{cases} C_{\text{C-GSM}} + C_F N_{ED}, \text{if } M = 1 \\ C_{\text{C-GSM}} + C_F N^M_{ED} \frac{(1 + M^{N_u})M^{N_u}}{2}, \text{else} \end{cases} \tag{18}$$

since $C^{N_u}_{N_t}(M^{N_u} - 1)^2/2$ EDs are calculated in the TAC set selection.

IV. Transmit antenna combination selection for the GSM system operating without channel state information

In this selection, the ABEP assisted TAC selection conceived for the HM-GSM system operating without CSI knowledge is investigated. Firstly, the ABEP analysis of

This work is licensed under a Creative Commons Attribution 3.0 License. For more information, see http://creativecommons.org/licenses/by/3.0/.

This article has been accepted for publication in a future issue of this journal, but has not been fully edited. Content may change prior to final publication. Citation information: DOI 10.1109/ACCESS.2018.2859794, IEEE Access

the GSM system is carried out. Then, its TAC selection is developed. Finally, a novel bit-to-TAC mapping approach is proposed for further improving the GSM system's performance.

A. ABEP Analysis of the GSM System

In this section, the ABEP performance of the GSM system is derived. Let us denote the transmit and receive signal of GSM by $\mathbf{x}_i$ and $\mathbf{x}_j$, respectively. Then the ABEP upper bound is given by

$$P_b = \sum_{\forall \mathbf{x}_i} \sum_{\forall \mathbf{x}_j \neq \mathbf{x}_i} \frac{d_{\mathbf{x}_i,\mathbf{x}_j} \bar{P}_e(\mathbf{x}_i \to \mathbf{x}_j)}{B2^B}, \tag{19}$$

where $\bar{P}_e(\mathbf{x}_i \to \mathbf{x}_j)$ is the Pairwise Error Probability (PEP) and $d_{\mathbf{x}_i,\mathbf{x}_j}$ is the number of bit errors associated with the corresponding PEP event. According to [24], $\bar{P}_e(\mathbf{x}_i \to \mathbf{x}_j)$ may be expressed as

$$\bar{P}_e(\mathbf{x}_i \to \mathbf{x}_j) = F(\bar{\zeta}) = \gamma(\bar{\varsigma}) \sum_{k=0}^{N_r-1} C^k_{N_r-1+k}[1-\gamma(\bar{\varsigma})]^k, \tag{20}$$

where $\gamma(\bar{\varsigma}) = \frac{1}{2}\left(1-\sqrt{\frac{\bar{\varsigma}/2}{1+\bar{\varsigma}/2}}\right)$ and $\bar{\varsigma}$ is the mean value of $\varsigma = ||\mathbf{H}(\mathbf{x}_i - \mathbf{x}_j)||^2_F / 2\sigma^2$ with $N_r = 1$. For the GSM system, assuming that the antenna indices of the transmit signal $\mathbf{x}_i$ and the estimated $\mathbf{x}_j$ are $(l_1, l_2, ..., l_{N_u})$ and $(\hat{l}_1, \hat{l}_2, ..., \hat{l}_{N_u})$, respectively, and the corresponding symbol vectors are $\mathbf{s} = [s_1, s_2, ..., s_{N_u}]^T$ and $\hat{\mathbf{s}} = [\hat{s}_1, \hat{s}_2, ..., \hat{s}_{N_u}]^T$. Then the value of $\bar{\varsigma}$ for the GSM system is given by

$$\bar{\varsigma} = \begin{cases} \frac{|s_1-\hat{s}_1|^2+\cdots+|s_{N_u}-\hat{s}_{N_u}|^2}{2\sigma^2}, \text{ if } m = N_u \\ \frac{|s_1-\hat{s}_1|^2+\cdots+|s_m-\hat{s}_m|^2+2(N_u-m)}{2\sigma^2}, \text{if } 0< m < N_u \\ \frac{2N_u}{2\sigma^2}, \text{if } m = 0 \end{cases}, \tag{21}$$

where m is the number of identical antenna indices between $(l_1, l_2, ..., l_{N_u})$ and $(\hat{l}_1, \hat{l}_2, ..., \hat{l}_{N_u})$. Based on the values of $\bar{\varsigma}$ obtained in Eq. (21), the ABEP of the GSM system can be evaluated using (19).

Observe from (21) that there are lots of identical $\bar{\varsigma}$ values and the number of different values of $\bar{\varsigma}$ is finite for a fixed constellation size M, N_r and SNR variance σ^2. Hence, the above ABEP expressions can be further simplified. Assuming that the GSM systems have n different values $\bar{\varsigma}$ as $\bar{\varsigma}_1$,...,$\bar{\varsigma}_n$, the corresponding PEP values $F(\bar{\varsigma}_1)$,...,$F(\bar{\varsigma}_n)$ can be obtained from (20), so that (19) can be represented as

$$\begin{aligned} P_b &= \frac{\sum_{t=1}^{\lambda_1} d^t_{\bar{\varsigma}_1} F(\bar{\varsigma}_1) + \sum_{t=1}^{\lambda_2} d^t_{\bar{\varsigma}_2} F(\bar{\varsigma}_2) + \cdots + \sum_{t=1}^{\lambda_n} d^t_{\bar{\varsigma}_2} F(\bar{\varsigma}_n)}{B2^B} \\ &= D(\bar{\varsigma}_1)F(\bar{\varsigma}_1) + D(\bar{\varsigma}_2)F(\bar{\varsigma}_2) + \cdots + D(\bar{\varsigma}_n)F(\bar{\varsigma}_n) \end{aligned} \tag{22}$$

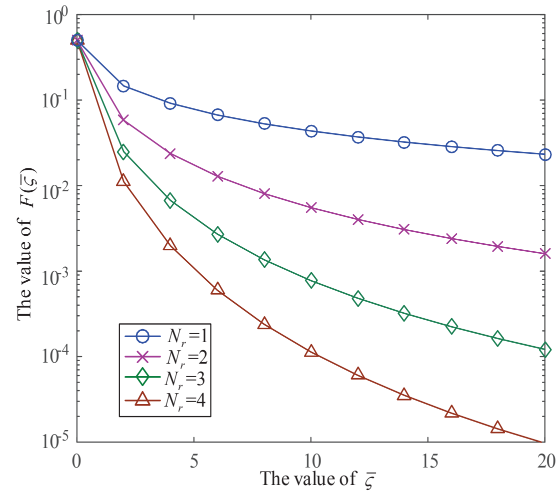

Fig. 2. The values of $F(\bar{\varsigma})$.

with

$$D(\bar{\varsigma}_p) = \sum_{t=1}^{\lambda_p} d^t_{\bar{\varsigma}_p} / B2^B, p = 1, ..., n,$$

$$\sum_{t=1}^{\lambda_1} d^t_{\bar{\varsigma}_1} + \cdots + \sum_{t=1}^{\lambda_n} d^t_{\bar{\varsigma}_n} = \sum_{i=1}^{2^B} \sum_{j=1}^{2^B} d(\mathbf{x}_i, \mathbf{x}_j) = 2^B \sum_{u=1}^{B} C^u_B u, \tag{23}$$

where λ_p $p \in \{1, ..., n\}$ is the total number of candidate $\bar{\zeta}_p$ for all the $\mathbf{x}_i$ and $\mathbf{x}_j$, while $d^t_{\bar{\varsigma}_p}$ is the corresponding Hamming Distance (HD), and $D(\bar{\varsigma}_p)$ is the Average HD (AHD) for the value $\bar{\zeta}_p$.

Next, AHD based TAC selection is developed. Since only the TACs are selected, we employ $M = 1$ for our GSM system for simplicity, so that Eq. (21) can be further simplified to

$$\bar{\varsigma} = \begin{cases} 0, \text{ if } m = N_u \\ \frac{2(N_u-m)}{2\sigma^2}, \text{if } 0< m < N_u \\ \frac{2N_u}{2\sigma^2}, \text{if } m = 0 \end{cases}. \tag{24}$$

As a result, there are a total of N_u different values $\bar{\varsigma}$ as $\bar{\varsigma}_1$,...,$\bar{\varsigma}_{N_u}$ as

$$\begin{array}{l} \bar{\varsigma}_1 = \frac{1}{\sigma^2}, m = N_u - 1 \\ \bar{\varsigma}_2 = \frac{2}{\sigma^2}, m = N_u - 2 \\ \vdots \\ \bar{\varsigma}_{N_u} = \frac{N_u}{\sigma^2}, m = 0 \end{array}. \tag{25}$$

Hence, the ABEP of the GSM system associated with $M = 1$ is dominated by the values of $\bar{\varsigma}_n$ and $F(\bar{\varsigma}_n)$. The relationship between $\bar{\varsigma}_n$ and $F(\bar{\varsigma}_n)$ is presented graphically in Fig. 2. Observe from Fig. 2 that we have

$$F(\bar{\varsigma}_1) >> F(\bar{\varsigma}_2) > \cdots > F(\bar{\varsigma}_{N_u}). \tag{26}$$

where $x >> y$ denotes the value of x is much larger than that of y. Hence, the associated optimization principle can be invoked for designing a GSM system having a small value of $D(\bar{\varsigma}_1)$. According to (23), the value of $D(\bar{\varsigma}_1)$ is dominated by two parts: the total number λ_1 of

This work is licensed under a Creative Commons Attribution 3.0 License. For more information, see http://creativecommons.org/licenses/by/3.0/.

This article has been accepted for publication in a future issue of this journal, but has not been fully edited. Content may change prior to final publication. Citation information: DOI 10.1109/ACCESS.2018.2859794, IEEE Access

candidate $\bar{\zeta}_1$ $(m = N_u - 1)$ and its corresponding HD of $d^t_{\bar{\varsigma}_1}$ $(t = 1, ..., \lambda_1)$. Next, the TAC selection aims for attaining a small value of λ_1 and $d^t_{\bar{\varsigma}_1}$ $(t = 1, ..., \lambda_1)$, which are introduced as follows.

B. TAC Selection

For each TAC $I_j, j \in [1, N_{\text{all}}]$, the set $\psi_j = \mathbb{I}_{\text{all}} \backslash I_j$ consists of N_u parts $\psi_j^{N_u-1}$, $\psi_j^{N_u-2}$ and ψ_j^0, where $\forall I_r \in \psi_j^m$ $m = 0, ..., N_u - 1$ indicates that there are m common indices between I_r and I_j, while $A \backslash B$ represents removing B from A. Next, the TAC selections invoked for specific antenna setups are introduced as follows.

1) TAC Selection for $N_t = 4, N_u = 2$:

Fig. 3 portrays the TAC selection for the case of $N_t = 4$ and $N_u = 2$. In this scenario, we have $\mathbb{I}_{\text{all}} = [(1,2),(1,3),(1,4),(2,3),(2,4)]$. For any two TACs from $\mathbb{I}_{\text{all}}$, the two TACs are connected by the curves seen in Fig. 3, if there are $N_u - 1$ common indices between the two TACs. As a result, the TAC selection problem has been transformed as to how we remove TACs having the lowest number of curves. For the case of $N_t = 4$ and $N_u = 2$, we have

$$\begin{array}{l} \underbrace{(1,2)}_{I_1} \rightarrow \psi_1^1 = \{\underbrace{(1,3)}_{I_2}, \underbrace{(1,4)}_{I_3}, \underbrace{(2,3)}_{I_4}, \underbrace{(2,4)}_{I_5}\}; \psi_1^0 = \{\underbrace{(3,4)}_{I_6}\} \\ \underbrace{(1,3)}_{I_2} \rightarrow \psi_2^1 = \{\underbrace{(1,2)}_{I_1}, \underbrace{(1,4)}_{I_3}, \underbrace{(2,3)}_{I_4}, \underbrace{(3,4)}_{I_6}\}; \psi_2^0 = \{\underbrace{(2,4)}_{I_5}\} \\ \underbrace{(1,4)}_{I_3} \rightarrow \psi_3^1 = \{\underbrace{(1,2)}_{I_1}, \underbrace{(1,3)}_{I_2}, \underbrace{(2,4)}_{I_5}, \underbrace{(3,4)}_{I_6}\}; \psi_3^0 = \{\underbrace{(2,3)}_{I_4}\} \end{array} . \tag{27}$$

Observe from Fig. 3 that by removing (I_1, ψ_1^0), (I_2, ψ_2^0) and (I_3, ψ_3^0), we can obtain a smaller value of λ_1.

2) TAC Selection for $N_t = 5, N_u = 2$:

Fig. 4 portrays the TAC selection for the case of $N_t = 5$ and $N_u = 2$. For the case of $N_t = 5$ and $N_u = 2$, we have $\mathbb{I}_{\text{all}} = [(1,2),(1,3),(1,4),(1,5),(2,3),(2,4),(2,5),(3,4),(3,5),(4,5)]$. $N = 8$ TACs should be selected from the set $\mathbb{I}_{\text{all}}$. For the case of $N_t = 5$ and $N_u = 2$, we have

$$\underbrace{(1,2)}_{I_1} \rightarrow \psi_1^0 = \{\underbrace{(3,4)}_{I_8}, \underbrace{(3,5)}_{I_9}, \underbrace{(4,5)}_{I_{10}}\}. \tag{28}$$

Observe from Fig. 4 that by removing (I_1, I_8), (I_1, I_9) and (I_1, I_{10}), we arrive at at a reduced value of λ_1.

$$\begin{array}{l} \psi_1^1 = \{(1,3),(1,4),(1,5),(2,3),(2,4),(2,5)\} \\ \psi_1^0 = \{(3,4),(3,5),(4,5)\} \end{array} . \tag{29}$$

Then we can get the TAC set as

$$\mathbb{I}_o = \{\underbrace{(1,3),(1,4),(1,5),(2,3),(2,4),(2,5)}_{\psi_1^1}, \underbrace{(3,4),(3,5)}_{\mathcal{I}_{\text{left}}}\}. \tag{30}$$

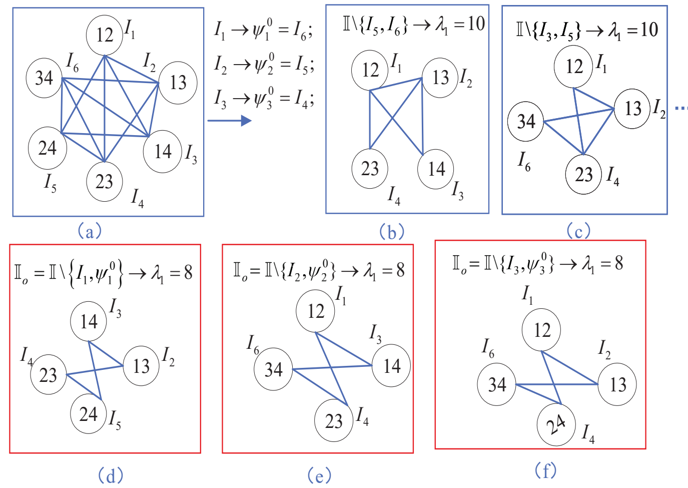

Fig. 3. The TAC selection for HM-GSM system having $N_t = 4$ and $N_u = 2$.

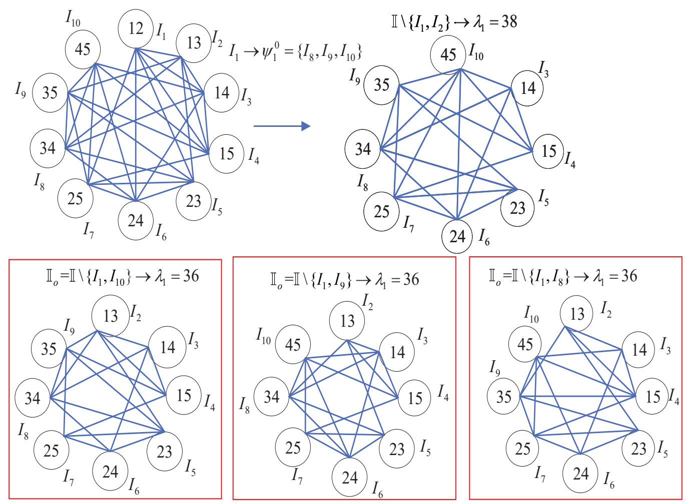

Fig. 4. The TAC selection for HM-GSM system having $N_t = 5$ and $N_u = 2$.

3) Generalized TAC Selection for $N_u = 2$:

Based on the above TAC selection examples, the generalized TAC selection design is introduced as follows.

Step 1: For the specific TAC $I_j, j \in [1, N_{\text{all}}]$, obtain the corresponding TAC set $\psi_j^{N_u-1}$, $\psi_j^{N_u-2}, ..., \psi_j^0$.

Step 2: Remove $N_{\text{all}} - N + 1$ TACs $\mathcal{I}_j$ from the TAC set $\psi_j^{N_u-2}, ..., \psi_j^0$ and obtain the $\mathcal{I}_{\text{left}} = \{\psi_j^{N_u-2}, ..., \psi_j^0\} \backslash \mathcal{I}_j$

Step 3: Obtain the final TAC set $\mathbb{I}_o = \{\psi_j^{N_u-1}, \mathcal{I}_{\text{left}}\}$.

Due to the associated symmetry, the TAC selection is the same for each I_j. For simplicity, we introduce the TAC selection process for $I_1 = [1, 2, ..., N_u]$ in detail as follows.

For the case of $N_u = 2$, the TAC set can be expressed

This work is licensed under a Creative Commons Attribution 3.0 License. For more information, see http://creativecommons.org/licenses/by/3.0/.

This article has been accepted for publication in a future issue of this journal, but has not been fully edited. Content may change prior to final publication. Citation information: DOI 10.1109/ACCESS.2018.2859794, IEEE Access

as

$$\mathbb{I}_{N_{\text{all}}} = \left\{ \begin{array}{l} \underbrace{(1,2),(1,3)\cdots(1,N_t)}_{N_t-1} \\ \underbrace{(2,3),(2,4)\cdots(2,N_t)}_{N_t-2} \\ \underbrace{(3,4),(3,5)\cdots(3,N_t)}_{N_t-3} \\ \vdots \\ \underbrace{(N_t-1,N_t)}_{1} \end{array} \right\}. \quad (31)$$

Firstly, for the TAC $I_1 = (1,2)$, we can obtain the corresponding set ψ_1^1 and ψ_1^0 as

$$\psi_1^1 = \left\{ \begin{array}{l} \underbrace{((1,3),\cdots(1,N_t)}_{N_t-2} \\ \underbrace{(2,3),\cdots(2,N_t)}_{N_t-2} \end{array} \right\}, \psi_1^0 = \left\{ \begin{array}{l} \underbrace{(3,4),\cdots(3,N_t)}_{N_t-3} \\ \vdots \\ \underbrace{(N_t-1,N_t)}_{1} \end{array} \right\} \quad (32)$$

Secondly, select $N-(N_t-2)^2$ TACs from ψ_1^0 as $\mathcal{I}_{\text{left}} \subset \psi_1^0$ and obtain the final TAC set as $\mathbb{I}_o = \{\psi_1^1, \mathcal{I}_{\text{left}}\}$.

4) Generalized TAC Selection for $N_u > 2$:

For the case of $N_u > 2$, there are a total of $C_{N_t}^{N_u}$ TACs. For the TAC $I_1 = (1,2,...,N_u)$, to obtain the set ψ_1^m, $m = 0,...,N_u-1$, we first choose the m indices from $I_1 = (1,2,...,N_u)$ and choose the left $N_u - m$ indices from $(N_u+1,...,N_t)$, hence there are a total number of $C_{N_u}^m C_{N_t-N_u}^{N_u-m}$ TACs in the ψ_1^m. The set $\psi_1^{N_u-1}$, $\psi_1^{N_u-2}$,...,ψ_1^0 can be obtain as follows

$$\psi_1^{N_u-1} = \left\{ \begin{array}{l} \underbrace{(1,2,...,(N_u-1),N_u+1),\cdots(1,2,...,N_t)}_{N_t-N_u} \\ \underbrace{(1,3...,N_u,N_u+1),\cdots(1,3,...,N_u,N_t)}_{N_t-N_u} \\ \vdots \\ \underbrace{(2,3...,N_u,N_u+1),\cdots(2,3,...,N_u,N_t)}_{N_t-N_u} \end{array} \right\}$$
$$\psi_1^{N_u-2} = \left\{ \begin{array}{l} \underbrace{(1,2,...,(N_u-1),N_u+1),\cdots(1,2,...,N_t)}_{N_t-N_u} \\ \vdots \\ \underbrace{(2,3...,N_u,N_u+1),\cdots(2,3,...,N_u,N_t)}_{N_t-N_u} \end{array} \right\}.$$
$$\vdots$$
$$\psi_1^0 = \left\{ \begin{array}{l} \underbrace{(N_u+1,\cdots 2N_u),\cdots(N_u+1,\cdots N_t)}_{N_t-2N_u+1} \\ \vdots \\ \underbrace{(N_t-N_u+1,\cdots,N_t)}_{N_t-N_u} \end{array} \right\} \quad (33)$$

Based on the generalized TAC selection principle, the final TAC set can be obtained as

$$\mathbb{I}_o = \{\psi_1^{N_u-1}, \mathcal{I}_{\text{left}}\} \quad (34)$$

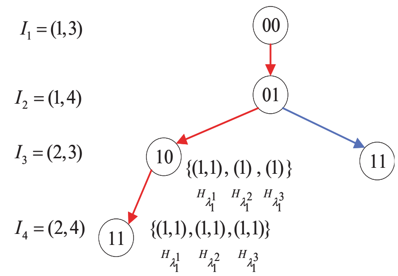

Fig. 5. Bit-to-TAC mapping for HM-GSM system having $N_t = 4$ and $N_u = 2$.

where $\mathcal{I}_{\text{left}}$ is the first $N - (C_{N_u}^1 C_{N_t-N_u}^1)$ values of the set $\psi_1^{\neq(N_u-1)} = \{\psi_1^{N_u-2}, \cdots \psi_1^0\}$

C. Bit-to-TAC Mapping

After obtaining the TAC set $\mathbb{I}_o$, bit-to-TAC mapping is the key issue to obtain small HD values of $d_{\bar{\varsigma}_1}^t$. The possible HDs between any two block of bits with length of B can be expressed as

$$\mathbb{H} = (\underbrace{1,...,1}_{C_B^1}, \underbrace{2,...,2}_{C_B^2}, ..., \underbrace{u,...,u}_{C_B^u}, ..., \underbrace{B}_{C_B^B}). \quad (35)$$

For each TAC $I_{o,i} \in \mathbb{I}_o$, $i = (1,2,...,N)$, there are λ_1^i TACs termed as $\psi_{o,i}^{N_u-1}$ having $N_u - 1$ common indices as $I_{o,i}$, resulting in λ_1^i HDs as $d_{\bar{\varsigma}_1}^1, d_{\bar{\varsigma}_1}^2, ..., d_{\bar{\varsigma}_1}^{\lambda_1^i}$. Assuming that $\mathbf{H}_{\lambda_1^i} = (d_{\bar{\varsigma}_1}^1, d_{\bar{\varsigma}_1}^2, ..., d_{\bar{\varsigma}_1}^{\lambda_1^i})$ denotes a set having λ_1^i elements of $\mathbb{H}$, $D_{\bar{\varsigma}_1}^i = \sum \mathbf{H}_{\lambda_1^i}$ represents the total number of common HDs between $I_{o,i}$ and $\psi_{o,i}^{N_u-1}$, we have

$$\begin{aligned} &\lambda_1 = \lambda_1^1 + \lambda_1^2 + \cdots + \lambda_1^N, \\ &D_{\bar{\varsigma}_1}^i = \sum \mathbf{H}_{\lambda_1^i} = \sum_{t=1}^{\lambda_1^i} d_{\bar{\varsigma}_1}^t, \\ &\sum_{t=1}^{\lambda_1} d_{\bar{\varsigma}_1}^t = \sum_{i=1}^{N} D_{\bar{\varsigma}_1}^i. \end{aligned} \quad (36)$$

Then the value of $D(\bar{\varsigma}_1)$ can be represented as

$$D(\bar{\varsigma}_1) = \frac{\sum_{i=1}^{N} D_{\bar{\varsigma}_1}^i}{B^{2B}}. \quad (37)$$

As a result, the bit-to-TAC mapping has to satisfy

$$\begin{aligned} &\min_{\mathbf{H}_{\lambda_1^i}} [D(\bar{\varsigma}_1)] \\ &s.t. \lambda_1 = \lambda_1^1 + \lambda_1^2 + \cdots + \lambda_1^N, \\ &D_{\bar{\varsigma}_1}^i = \sum \mathbf{H}_{\lambda_1^i}, \mathbf{H}_{\lambda_1^i} \in \mathbb{H} \end{aligned} \quad (38)$$

where λ_1 can be obtained in Section IV-B. Next, the bit-to-TAC mapping of $N_t = 4, N_u = 2$ and $N_t = 5, N_u = 2$ is introduced first, then it is extended to the generalized cases.

This work is licensed under a Creative Commons Attribution 3.0 License. For more information, see http://creativecommons.org/licenses/by/3.0/.

This article has been accepted for publication in a future issue of this journal, but has not been fully edited. Content may change prior to final publication. Citation information: DOI 10.1109/ACCESS.2018.2859794, IEEE Access

1) Bit-to-TAC Mapping for $N_t = 4, N_u = 2$:

Fig. 5 presents the bit-to-TAC mapping for the case of $N_t = 4$ and $N_u = 2$. In this case, we have $B = 2$ and

$$\begin{aligned}
\underbrace{(1,3)}_{I_{o,1}} &\rightarrow \psi^1_{o,1} = \{(1,4),(2,3)\} \\
\underbrace{(1,4)}_{I_{o,2}} &\rightarrow \psi^1_{o,2} = \{(1,4),(2,4)\} \\
\underbrace{(2,3)}_{I_{o,3}} &\rightarrow \psi^1_{o,3} = \{(1,3),(2,4)\} \\
\underbrace{(2,4)}_{I_{o,4}} &\rightarrow \psi^1_{o,4} = \{(1,4),(2,3)\}
\end{aligned}. \tag{39}$$

According to (35)-(38), the HD set $\mathbf{H}_{\lambda_1^i}$ can be obtained by

$$\begin{aligned}
\underbrace{(1,3)}_{I_{o,1}} &\rightarrow \lambda_1^1 = 2 \rightarrow \mathbf{H}_{\lambda_1^1} = (1,1) \\
\underbrace{(1,4)}_{I_{o,2}} &\rightarrow \lambda_1^2 = 2 \rightarrow \mathbf{H}_{\lambda_1^2} = (1,1) \\
\underbrace{(2,3)}_{I_{o,3}} &\rightarrow \lambda_1^3 = 2 \rightarrow \mathbf{H}_{\lambda_1^3} = (1,1) \\
\underbrace{(2,4)}_{I_{o,4}} &\rightarrow \lambda_1^4 = 2 \rightarrow \mathbf{H}_{\lambda_1^4} = (1,1)
\end{aligned}. \tag{40}$$

As seen from Fig. 5, the bit-to-TAC mapping can be obtained as

$$00 \rightarrow (1,3), 01 \rightarrow (1,4), 10 \rightarrow (2,3), 11 \rightarrow (2,4). \tag{41}$$

2) Bit-to-TAC Mapping for $N_t = 5, N_u = 2$:

Fig. 6 presents the bit-to-TAC mapping for the case of $N_t = 5$ and $N_u = 2$. For the scenario of $N_t = 5$ and $N_u = 2$, we have $B = 3$ and

$$\begin{aligned}
\underbrace{(1,4)}_{I_{o,1}} &\rightarrow \psi^1_{o,1} = \{(1,3),(1,5),(2,4),(3,4)\} \\
\underbrace{(1,5)}_{I_{o,2}} &\rightarrow \psi^1_{o,2} = \{(1,3),(1,4),(2,5),(3,5)\} \\
\underbrace{(2,4)}_{I_{o,3}} &\rightarrow \psi^1_{o,3} = \{(1,4),(2,3),(2,5),(3,4)\} \\
\underbrace{(2,5)}_{I_{o,4}} &\rightarrow \psi^1_{o,4} = \{(1,5),(2,3),(2,4),(3,5)\} \\
\underbrace{(2,3)}_{I_{o,5}} &\rightarrow \psi^1_{o,5} = \{(1,3),(2,4),(2,5),(3,4),(3,5)\} \\
\underbrace{(1,3)}_{I_{o,6}} &\rightarrow \psi^1_{o,6} = \{(1,4),(1,5),(2,3),(3,4),(3,5)\} \\
\underbrace{(3,4)}_{I_{o,7}} &\rightarrow \psi^1_{o,7} = \{(1,3),(1,4),(2,3),(2,4),(3,5)\} \\
\underbrace{(3,5)}_{I_{o,8}} &\rightarrow \psi^1_{o,8} = \{(1,3),(1,5),(2,3),(2,5),(3,4)\}
\end{aligned}. \tag{42}$$

According to (36)-(38), the set $\mathbf{H}_{\lambda_1^i}$ for each TAC $I_{o,i}$ can be expressed as

$$\begin{aligned}
\underbrace{(1,4)}_{I_{o,1}} &\rightarrow \lambda_1^1 = 4 \rightarrow \mathbf{H}_{\lambda_1^1} = (1,1,1,2) \\
\underbrace{(1,5)}_{I_{o,2}} &\rightarrow \lambda_1^2 = 4 \rightarrow \mathbf{H}_{\lambda_1^2} = (1,1,1,2) \\
\underbrace{(2,4)}_{I_{o,3}} &\rightarrow \lambda_1^3 = 4 \rightarrow \mathbf{H}_{\lambda_1^3} = (1,1,1,2) \\
\underbrace{(2,5)}_{I_{o,4}} &\rightarrow \lambda_1^4 = 4 \rightarrow \mathbf{H}_{\lambda_1^4} = (1,1,1,2) \\
\underbrace{(1,3)}_{I_{o,5}} &\rightarrow \lambda_1^5 = 5 \rightarrow \mathbf{H}_{\lambda_1^5} = (1,1,1,2,2) \\
\underbrace{(2,3)}_{I_{o,6}} &\rightarrow \lambda_1^6 = 5 \rightarrow \mathbf{H}_{\lambda_1^6} = (1,1,1,2,2) \\
\underbrace{(3,4)}_{I_{o,7}} &\rightarrow \lambda_1^7 = 5 \rightarrow \mathbf{H}_{\lambda_1^7} = (1,1,1,2,2) \\
\underbrace{(3,5)}_{I_{o,8}} &\rightarrow \lambda_1^8 = 5 \rightarrow \mathbf{H}_{\lambda_1^8} = (1,1,1,2,2)
\end{aligned}. \tag{43}$$

Hence, the general bit-to-TAC mapping principle is based on the values of $\mathbf{H}_{\lambda_1^i}$ in (43), which is detailed as follows.

Initialize $(1,3) \rightarrow 000, (1,4) \rightarrow 001$.

Step 1: The bit-to-TAC mapping begins from $\psi^1_{o,1}$. Since the TAC mapping should satisfy Eq. (43), we have $(1,5) \in \{010, 011, 100, 101\}$.

Step 2: If $(1,5) \rightarrow 010$, we have $\mathbf{H}_{\lambda_1^1} = (1,2)$ and $\mathbf{H}_{\lambda_1^2} = (1,2)$. According to Eq. (43), we have $(2,4),(3,4) \in \{101, 011\}$ and $(2,5),(3,5) \in \{011, 110\}$. The bits set $\{011, 101, 110\}$ should be mapped to four TACs $(2,4),(3,4),(2,5),(3,5)$, resulting in mapping errors. Hence, $'010'$ cannot be mapped to $(1,5)$.

Step 3: If $(1,5) \rightarrow 011$, we have $\mathbf{H}_{\lambda_1^1} = (1,1)$ and $\mathbf{H}_{\lambda_1^2} = (1,2)$. According to (42)-(43), we have $(2,5),(3,5) \in \{010, 111\}$ and the following expressions can be formulated

$$\begin{aligned}
\underbrace{(1,4)}_{001} &\rightarrow \psi^1_{o,1} = \{\underbrace{(1,3)}_{000\rightarrow 1}, \underbrace{(1,5)}_{011\rightarrow 1}, (2,4),(3,4)\} \\
\underbrace{(1,5)}_{011} &\rightarrow \psi^1_{o,2} = \{\underbrace{(1,3)}_{000\rightarrow 2}, \underbrace{(1,4)}_{001\rightarrow 1}, \underbrace{(2,5)}_{010/111}, \underbrace{(3,5)}_{010/111}\}
\end{aligned}. \tag{44}$$

Step 4: The bit-to-TAC mapping continues from the TAC $(2,5)$. If $(2,5) \rightarrow 010$, we have

$$\underbrace{(2,5)}_{010} \rightarrow \psi^1_{o,4} = \{\underbrace{(1,5)}_{011\rightarrow 1}, \underbrace{(2,3)}_{110\rightarrow 1}, \underbrace{(2,4)}_{000\rightarrow 1}, \underbrace{(3,5)}_{111\rightarrow 2}\}. \tag{45}$$

Then we should have $(2,4) \rightarrow 000$ in order to satisfy Eq. (43), which is the same as $(1,3) \rightarrow 000$. Hence, $(2,5)$ cannot be mapped to 010 and the bit-to-TAC mapping starts from $(2,5) \rightarrow 111$ as

$$\underbrace{(2,5)}_{111} \rightarrow \psi^1_{o,4} = \{\underbrace{(1,5)}_{011\rightarrow 1}, \underbrace{(2,3)}_{110/101}, \underbrace{(2,4)}_{110/101}, \underbrace{(3,5)}_{010\rightarrow 2}\}. \tag{46}$$

Step 5: According to (46), the bit-to-TAC mapping continues from the TAC $(2,4)$. If $(2,4) \rightarrow 110$, the HD

This work is licensed under a Creative Commons Attribution 3.0 License. For more information, see http://creativecommons.org/licenses/by/3.0/.

This article has been accepted for publication in a future issue of this journal, but has not been fully edited. Content may change prior to final publication. Citation information: DOI 10.1109/ACCESS.2018.2859794, IEEE Access

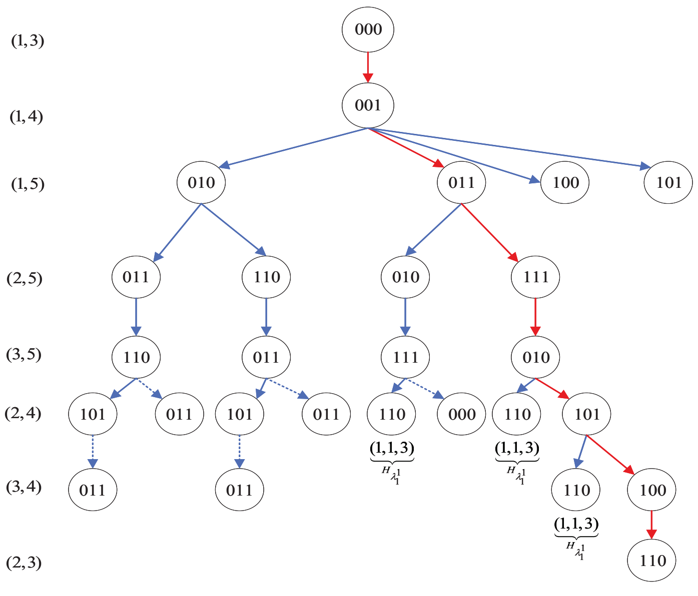

Fig. 6. Bit-to-TAC mapping for HM-GSM system having $N_t = 5$ and $N_u = 2$.

between $(2,4)$ and $(1,4)$ is 3, so that we have $(2,4) \to 101$ and the following expressions can be formulated

$$\begin{aligned} &\underbrace{(2,5)}_{111} \to \psi_{o,4}^{1} = \{\underbrace{(1,5)}_{011\to1}, \underbrace{(2,3)}_{110\to1}, \underbrace{(2,4)}_{101\to1}, \underbrace{(3,5)}_{010\to2}\} \\ &\underbrace{(1,4)}_{001} \to \psi_{o,1}^{1} = \{\underbrace{(1,3)}_{000\to1}, \underbrace{(1,5)}_{011\to1}, \underbrace{(2,4)}_{101\to1}, \underbrace{(3,4)}_{100\to2}\} \\ &\underbrace{(2,4)}_{101} \to \psi_{o,3}^{1} = \{\underbrace{(1,4)}_{001\to1}, \underbrace{(2,3)}_{110\to2}, \underbrace{(2,5)}_{111\to1}, \underbrace{(3,4)}_{100\to1}\} \end{aligned} . \tag{47}$$

Finally, as shown in Fig. 6, the bit-to-TAC mapping for the case of $N_t = 5$ and $N_u = 2$ is given by

$$\begin{aligned} &000 \to (1,3), 001 \to (1,4), 010 \to (3,5), 011 \to (1,5) \\ &100 \to (3,4), 101 \to (2,4), 110 \to (2,3), 111 \to (2,5) \end{aligned} . \tag{48}$$

3) Bit-to-TAC Mapping for Generalized Cases:

Based on the bit-to-TAC mapping of the above specific examples, the generalized bit-to-TAC mapping is formulated as follows.

Step 1: Obtain the TAC set $\mathbb{I}_o$ and the HD set $\mathbb{H}$ according to (34) and (38).

Step 2: For each TAC $I_{o,i} \in \mathbb{I}_o$, obtain the set $\psi_{o,i}^{N_u-1}$ and the value λ_1^i according to (34).

Step 3: Obtain the HD set $\mathbf{H}_{\lambda_1^i}$ according to (38).

Step 4: Complete the bit-to-TAC mapping based on $I_{o,i} \in \mathbb{I}_o$, $\psi_{o,i}^{N_u-1}$, $\mathbf{H}_{\lambda_1^i}$ with $D_{\bar{\varsigma}_1}^{i}$.

Assuming that $\mathbb{B} = \{\mathbf{b}_1, ..., \mathbf{b}_N\}$ is the set of information bits, the bit-to-TAC mapping can be detailed as in Algorithm 1. As shown in Algorithm 1, there are lots of mapping options, which have the smallest value $d_{\lambda_1^i}^{\min}$. In fact, we only have to find a single appropriate mapping, hence the complexity of the bit-to-TAC mapping is determined by $\mathbb{I}_o$ and by the specific technique we select for mapping. Taking $N_t = 6$ and $N_u = 2$ as an example, we have $\mathbb{I}_o = \{(1,3),(1,4),(1,5),(1,6),(2,3),(2,4),(2,5),(2,6)\}$,

---

Algorithm 1 Bit-to-TAC mapping based the obtained TAC set $\mathbb{I}_o$

Input: $\mathbb{I}_o$, $\psi_{o,i}^{N_u-1}$, λ_1^i $\mathbf{H}_{\lambda_1^i}$, $i = 1, ..., N$, $D_{\bar{\varsigma}_1}^{i}$, $\mathbf{b}_{o,1} = \mathbf{b}_1$, $\mathbf{b}_{o,2} = \mathbf{b}_2$ $D_{\max}^i = \max(\mathbf{H}_{\lambda_1^i})$ $\mathcal{H}_{\lambda_1^i} = \phi$.

Output: $\hat{\mathbf{b}}$.

For the TAC $I_{o,3}$, obtain the possible bits set as $\mathbb{B}_{o,3}$ with number of $n_{o,3}$;
for $t_3 \in (1, n_{o,3})$ **do**
  $\mathbf{b}_{o,3} = \mathbb{B}_{o,3}^{t_3}$, $\mathbb{B}_{o,3}^{t_3}$ is the t_3-th element of $\mathbb{B}_{o,3}$.
  Update $\mathcal{H}_{\lambda_1^1}$, $\mathcal{H}_{\lambda_1^2}$, $\mathcal{H}_{\lambda_1^3}$, where $\mathcal{H}_{\lambda_1^i}$ denotes the HDs between two TACs inside the set $\psi_{o,i}^{N_u-1}$.
  if $\max(\mathcal{H}_{\lambda_1^i}) > D_{\max}^i \ || \sum \mathcal{H}_{\lambda_1^i} > D_{\bar{\varsigma}_1}^{i}$ **then**
    break;
  else
    $\mathbf{b}_{o,3} = \mathbb{B}_{o,3}^{t_3}$
  end if
  For the TAC $I_{o,4}$, obtain the possible bits set as $\mathbb{B}_{o,4}$ with number of $n_{o,4}$;
  for $t_4 \in (1, n_{o,4})$ **do**
    $\mathbf{b}_{o,4} = \mathbb{B}_{o,4}^{t_4}$.
    Update $\mathcal{H}_{\lambda_1^1}$, $\mathcal{H}_{\lambda_1^2}$, $\mathcal{H}_{\lambda_1^3}$ and $\mathcal{H}_{\lambda_1^4}$.
    if $\max(\mathcal{H}_{\lambda_1^i}) > D_{\max}^i \ || \sum \mathcal{H}_{\lambda_1^i} > D_{\bar{\varsigma}_1}^{i}$ **then**
      break;
    else
      $\mathbf{b}_{o,4} = \mathbb{B}_{o,4}^{t_4}$
    end if
  end for
  Get the possible bits set $\mathbb{B}_{o,5}$ with number of $n_{o,5}$;
  for $t_5 \in (1, n_{o,5})$ **do**
    ...
  end for
  ...
  Get the possible bits set $\mathbb{B}_{o,N}$ with number of $n_{o,N}$;
  for $t_N \in (1, n_{o,N})$ **do**
    ...
  end for
end for
$\hat{\mathbf{b}} = \{\mathbf{b}_1, \mathbf{b}_2, \mathbb{B}_{o,3}^{t_3}, \mathbb{B}_{o,3}^{t_4}, ..., \mathbb{B}_{o,N}^{t_N}\}$

---

then the bit-to-TAC mapping can be found without any extra complexity as

$$\begin{aligned} &(1,3) \to 000, (1,4) \to 001, (1,5) \to 010, (1,6) \to 011 \\ &(2,3) \to 100, (2,4) \to 101, (2,5) \to 110, (2,6) \to 111. \end{aligned} \tag{49}$$

In order to provide further insights, we compare the AHD of the proposed HM-GSM system to that of the C-GSM system in Table IV. Observe from Table IV that the proposed HM-GSM scheme is capable of attaining a significantly lower AHD $D(\bar{\varsigma}_1)$ than the C-GSM system.

V. Enhanced High Throughput GSM

In the above section, we have analyzed how to choose an optimal TAC set from the entire TAC set space, which is capable of providing a performance gain over the C-GSM system. In this section we discuss, how to exploiting the remaining TACs to increase the throughput.

This work is licensed under a Creative Commons Attribution 3.0 License. For more information, see http://creativecommons.org/licenses/by/3.0/.

This article has been accepted for publication in a future issue of this journal, but has not been fully edited. Content may change prior to final publication. Citation information: DOI 10.1109/ACCESS.2018.2859794, IEEE Access

TABLE VI
AHD COMPARISONS BETWEEN THE PROPOSED HM-GSM AND C-GSM SYSTEMS

Scheme	bit-to-TAC mapping	λ_1	$\sum_{t=1}^{\lambda_1} d_{\bar{\varsigma}_1}$	$D(\bar{\varsigma}_1)$
$N_t = 4, N_u = 2$				
C-GSM	$00 \rightarrow (1,2), 01 \rightarrow (2,3)$ $10 \rightarrow (1,3), 11 \rightarrow (1,4)$	10	14	1.75
HM-GSM	$00 \rightarrow (1,3), 01 \rightarrow (1,4)$ $10 \rightarrow (2,3), 11 \rightarrow (2,4)$	8	8	1
$N_t = 5, N_u = 2$				
C-GSM	$000 \rightarrow (1,4), 001 \rightarrow (2,3)$ $010 \rightarrow (2,5), 011 \rightarrow (3,4)$ $100 \rightarrow (3,5), 101 \rightarrow (4,5)$ $110 \rightarrow (2,4), 111 \rightarrow (1,5)$	38	76	3.17
HM-GSM	$000 \rightarrow (1,3), 001 \rightarrow (1,4)$ $010 \rightarrow (3,5), 011 \rightarrow (1,5)$ $100 \rightarrow (3,4), 101 \rightarrow (2,4)$ $110 \rightarrow (2,3), 111 \rightarrow (2,5)$	36	48	2
$N_t = 5, N_u = 3$				
C-GSM	$000 \rightarrow (1,2,3), 001 \rightarrow (1,2,4)$ $010 \rightarrow (1,4,5), 011 \rightarrow (2,3,5)$ $100 \rightarrow (2,3,4), 101 \rightarrow (1,3,5)$ $110 \rightarrow (1,2,5), 111 \rightarrow (1,3,4)$	38	76	3.17
HM-GSM	$000 \rightarrow (1,2,4), 001 \rightarrow (1,3,4)$ $010 \rightarrow (1,4,5), 011 \rightarrow (1,3,5)$ $100 \rightarrow (2,4,5), 101 \rightarrow (2,3,4)$ $110 \rightarrow (1,2,5), 111 \rightarrow (2,3,5)$	36	48	2

A. Proposed E-HT-GSM System

In the C-GSM system, only $N = 2^{\lfloor \log_2(C_{N_t}^{N_u}) \rfloor}$ TACs represent antenna index, while the remaining $C_{N_t}^{N_u} - N$ TACs are wasted. Here we propose reusing the remaining $(2^{\log_2(N)+1} - C_{N_t}^{N_u})$ TACs to convey an extra bit per time slot. The detailed process of the proposed E-HT-GSM is as follows.

Step 1: Determine the number of bits that the conventional TAC index conveys as

$$R_c = \lfloor \log_2(C_{N_t}^{N_u}) \rfloor \tag{50}$$

Step 2: Extend the number of bits conveyed to

$$R_p = \lfloor \log_2(C_{N_t}^{N_u}) \rfloor + 1. \tag{51}$$

Then the total number of TAC required by the proposed E-HT-GSM scheme becomes $N' = 2^{R_p}$.

Step 3: Naturally, we can only arrange for R_p bits be conveyed, if $(N' - C_{N_t}^{N_u})$ TACs are reused randomly and distinguishing rotated phase θ is employed for the reused TACs. The extended TAC set becomes $\mathbb{I}_{\text{high}} = [\mathbb{I}_{\text{all}}, \mathbb{I}_{\text{repeat}}]$.

Step 4: GSM mapping utilizing the extended TAC set $\mathbb{I}_{\text{high}}$.

Let us consider $N_t = 4$ for example, then the set of legitimate TACs for $N_t = 4$ is expressed as

$$\mathbb{I}_{\text{all}} = \left\{ \begin{bmatrix} 1 \\ 1 \\ 0 \\ 0 \end{bmatrix}, \begin{bmatrix} 1 \\ 0 \\ 1 \\ 0 \end{bmatrix}, \begin{bmatrix} 1 \\ 0 \\ 0 \\ 1 \end{bmatrix}, \begin{bmatrix} 0 \\ 1 \\ 1 \\ 0 \end{bmatrix}, \begin{bmatrix} 0 \\ 1 \\ 0 \\ 1 \end{bmatrix}, \begin{bmatrix} 0 \\ 0 \\ 1 \\ 1 \end{bmatrix} \right\}. \tag{52}$$

When reusing the two TACs $[1100]^T$ and $[0011]^T$, the repeated TACs are given by

$$\mathbb{I}_{\text{repeat}} = \left\{ \begin{bmatrix} 1 \\ 1 \\ 0 \\ 0 \end{bmatrix} e^{j\theta} \begin{bmatrix} 0 \\ 0 \\ 1 \\ 1 \end{bmatrix} e^{j\theta} \right\}. \tag{53}$$

According to (20) and (21), the extended TAC set is given by

$$\begin{aligned} \mathbb{I}_{\text{high}} = \Bigg\{ & \begin{bmatrix} 1 \\ 1 \\ 0 \\ 0 \end{bmatrix}, \begin{bmatrix} 1 \\ 0 \\ 1 \\ 0 \end{bmatrix}, \begin{bmatrix} 1 \\ 0 \\ 0 \\ 1 \end{bmatrix}, \begin{bmatrix} 0 \\ 1 \\ 1 \\ 0 \end{bmatrix}, \\ & \begin{bmatrix} 0 \\ 1 \\ 0 \\ 1 \end{bmatrix}, \begin{bmatrix} 0 \\ 0 \\ 1 \\ 1 \end{bmatrix}, \begin{bmatrix} e^{j\theta} \\ e^{j\theta} \\ 0 \\ 0 \end{bmatrix}, \begin{bmatrix} 0 \\ 0 \\ e^{j\theta} \\ e^{j\theta} \end{bmatrix} \Bigg\}. \end{aligned} \tag{54}$$

At the receiver, the ML detector and a range of low-complexity detectors designed for C-GSM systems can also be applied to the proposed E-HT-GSM systems.

B. The Optimization of θ

In this section, the value of θ is optimized by maximizing the Minimum Distance (MD) [42] associated with θ between the pair of E-HT-GSM symbols. Assuming that $\mathbf{x}_i$ and $\mathbf{x}_j$ are the transmit and estimated E-HT-GSM symbols, respectively, the MD between $\mathbf{x}_i$ and $\mathbf{x}_j$ can be expressed as

$$\delta_{\min}(\mathbf{x}_i, \mathbf{x}_j) = \min_{\mathbf{x}_i, \mathbf{x}_j} \det(\mathbf{x}_i - \mathbf{x}_j)(\mathbf{x}_i - \mathbf{x}_j)^H. \tag{55}$$

The optimization principle is based on maximizing the value of $\delta_{\min}(\mathbf{x}_i, \mathbf{x}_j)$. For simplicity, let us consider $N_u = 2$ for example. Specifically, the calculation is based on four scenarios:

1) Both $\mathbf{x}_i$ and $\mathbf{x}_j$ are independent of θ. In this case, the value of $\delta_{\min}(\mathbf{x}_i, \mathbf{x}_j)$ is independent of θ as well;
2) Both $\mathbf{x}_i$ and $\mathbf{x}_j$ are associated with the θ. In this case, the calculation is the same as the scenario 1);
3) $\mathbf{x}_i$ is independent of θ and $\mathbf{x}_j$ is associated with θ;
4) $\mathbf{x}_i$ is associated with θ and $\mathbf{x}_j$ is independent of θ.

The calculation process of scenario 3) and scenario 4) is the same due to their symmetry. As a result, we can focus on scenario 3) for our analysis. Assuming that the TAC and symbol vectors of $\mathbf{x}_i$ and $\mathbf{x}_j$ are given as (l_1, l_2), $\mathbf{s} = [s_1, s_2]^T$, and $(\hat{l}_1, \hat{l}_2)$, $\hat{\mathbf{s}} = [\hat{s}_1, \hat{s}_2]^T$, respectively, the value of $\delta_{\min}(\mathbf{x}_i, \mathbf{x}_j)$ can be calculated for three independent cases.

Case 1: All the activate antenna indices of $\mathbf{x}_i$ and $\mathbf{x}_j$ are the same. Assuming $l_1 = \hat{l}_1 = 1$, $l_2 = \hat{l}_2 = 2$, $\mathbf{x}_i =$

This work is licensed under a Creative Commons Attribution 3.0 License. For more information, see http://creativecommons.org/licenses/by/3.0/.

This article has been accepted for publication in a future issue of this journal, but has not been fully edited. Content may change prior to final publication. Citation information: DOI 10.1109/ACCESS.2018.2859794, IEEE Access

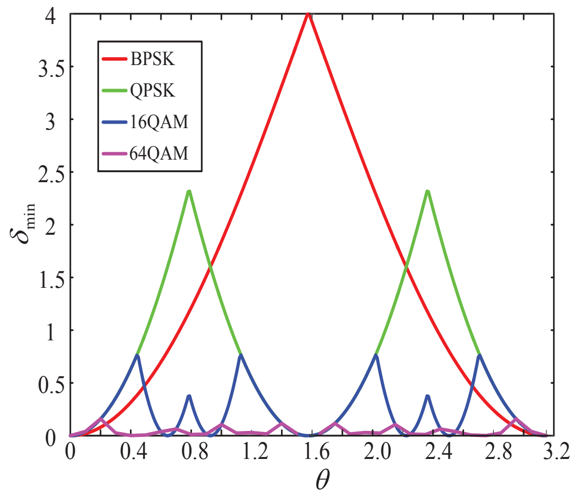

Fig. 7. The values of $\delta_{\min}(\mathbf{x}_i, \mathbf{x}_j)$ for different modulation orders.

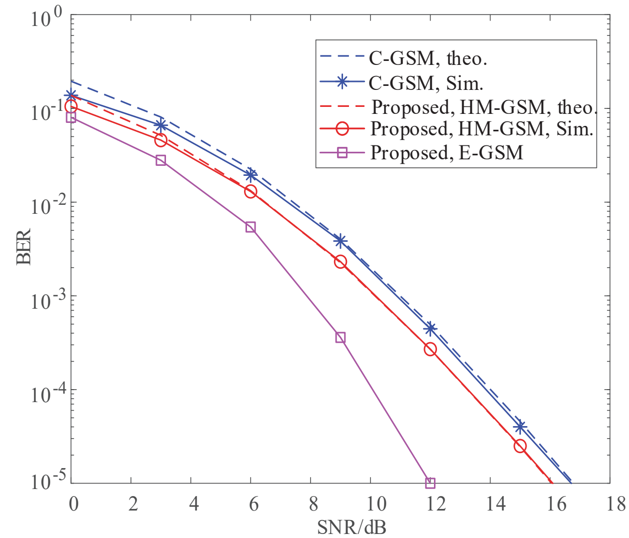

Fig. 8. Performance comparison of the proposed schemes and of the conventional GSM systems using $N_t = 4, N_r = 4, N_u = 2$ and $M = 1$ at 2 bits/symbol.

$[s_1 \quad s_2 \quad \mathbf{0}_{2\times(N_t-2)}]^T$, and $\mathbf{x}_j = [\hat{s}_1 \quad \hat{s}_2 \quad \mathbf{0}_{2\times(N_t-2)}]^T e^{j\theta}$ for example, the MD between $\mathbf{x}_i$ and $\mathbf{x}_j$ obeys

$$\begin{aligned}\delta_{\min}(\mathbf{x}_i, \mathbf{x}_j) &= \min_{\mathbf{x}_i, \mathbf{x}_j} \det(\mathbf{x}_i - \mathbf{x}_j)(\mathbf{x}_i - \mathbf{x}_j)^H \\ &= \min_{s_1, \hat{s}_1, s_2, \hat{s}_2} \det(s_1 - \hat{s}_1 e^{j\theta} \quad s_2 - \hat{s}_2 e^{j\theta} \quad \mathbf{0}_{2\times(N_t-2)}) \\ &\quad \times (s_1 - \hat{s}_1 e^{j\theta} \quad s_2 - \hat{s}_2 e^{j\theta} \quad \mathbf{0}_{2\times(N_t-2)})^H \\ &= \min_{s_1, \hat{s}_1, s_2, \hat{s}_2} \det(||s_1||^2 + ||s_2||^2 + ||\hat{s}_1||^2 + ||\hat{s}_2||^2 \\ &\quad - (s_1\hat{s}_1^* + s_2\hat{s}_2^*)e^{j\theta} - (s_1^*\hat{s}_1 + s_2^*\hat{s}_2)e^{j\theta}). \quad (56)\end{aligned}$$

Case 2: Only a single activated antenna index of $\mathbf{x}_i$ and $\mathbf{x}_j$ is the same. Assuming $s1 = 1, \hat{l}_1 = 2$, $l_2 = 1, \hat{l}_2 = 3$, $\mathbf{x}_i = [s_1 \quad s_2 \quad \mathbf{0}_{2\times(N_t-2)}]^T$, and $\mathbf{x}_j = [\hat{s}_1 \quad 0 \quad \hat{s}_2 \quad \mathbf{0}_{2\times(N_t-3)}]^T e^{j\theta}$ for example, the MD between $\mathbf{x}_i$ and $\mathbf{x}_j$ obeys

$$\begin{aligned}\delta_{\min}(\mathbf{x}_i, \mathbf{x}_j) &= \min_{\mathbf{x}_i, \mathbf{x}_j} \det(\mathbf{x}_i - \mathbf{x}_j)(\mathbf{x}_i - \mathbf{x}_j)^H \\ &= \min_{s_1, \hat{s}_1, s_2, \hat{s}_2} \det(s_1 - \hat{s}_1 e^{j\theta} \quad s_2 \quad -\hat{s}_2 e^{j\theta} \quad \mathbf{0}_{2\times(N_t-2)}) \\ &\quad \times (s_1 - \hat{s}_1 e^{j\theta} \quad s_2 \quad -\hat{s}_2 e^{j\theta} \quad \mathbf{0}_{2\times(N_t-3)})^H \\ &= \min_{s_1, \hat{s}_1, s_2, \hat{s}_2} \det(||s_1||^2 + ||s_2||^2 + ||\hat{s}_1||^2 + ||\hat{s}_2||^2 \\ &\quad - s_1\hat{s}_1^* e^{j\theta} + s_1^*\hat{s}_1 e^{j\theta}). \quad (57)\end{aligned}$$

Case 3: None of the activated antenna indices are the same. Considering $l_1 = 1, \hat{l}_1 = 2$, $l_2 = 3, \hat{l}_2 = 4$, $\mathbf{x}_i = \left(s_1 \quad s_2 \quad \mathbf{0}_{2\times(N_t-2)}\right)$, and $\mathbf{x}_j = \left(0 \quad 0 \quad \hat{s}_1 \quad \hat{s}_2 \quad \mathbf{0}_{2\times(N_t-4)}\right) e^{j\theta}$ for example, the MD between $\mathbf{x}_i$ and $\mathbf{x}_j$ obeys

$$\begin{aligned}\delta_{\min}(\mathbf{x}_i, \mathbf{x}_j) &= \min_{\mathbf{x}_i, \mathbf{x}_j} \det(\mathbf{x}_i - \mathbf{x}_j)(\mathbf{x}_i - \mathbf{x}_j)^H \\ &= \min_{s_1, \hat{s}_1, s_2, \hat{s}_2} \det(s_1 \quad s_2 \quad -\hat{s}_1 e^{j\theta} \quad -\hat{s}_2 e^{j\theta} \quad \mathbf{0}_{2\times(N_t-4)}) \\ &\quad \times (s_1 \quad s_2 \quad -\hat{s}_1 e^{j\theta} \quad -\hat{s}_2 e^{j\theta} \quad \mathbf{0}_{2\times(N_t-4)})^H \\ &= \min_{s_1, \hat{s}_1, s_2, \hat{s}_2} \det(||s_1||^2 + ||s_2||^2 + ||\hat{s}_1||^2 + ||\hat{s}_2||^2). \quad (58)\end{aligned}$$

As a result, the values of $\delta_{\min}(\mathbf{x}_i, \mathbf{x}_j)$ for the three cases can be summarized as (59), which is on the top of next page. According to (59), we have

$$\begin{aligned}\delta_{\min}(\mathbf{x}_i, \mathbf{x}_j) = \min_{x_{ij}, \hat{x}_{ij}} \det(&||s_1||^2 + ||s_2||^2 + ||\hat{s}_1||^2 + ||\hat{s}_2||^2 \\ &- (s_1\hat{s}_1^* + s_2\hat{s}_2^*)e^{j\theta} - (s_1^*\hat{s}_1 + s_2^*\hat{s}_2)e^{j\theta}). \quad (60)\end{aligned}$$

To provide further insights, Fig. 7 shows the value of $\delta_{\min}(\mathbf{x}_i, \mathbf{x}_j)$ in (60) for BPSK, QPSK, 16 QAM and 64-QAM in conjunction with different θ. If $\theta \in [0, \pi/2]$, as seen from Fig. 7, θ can be optimized by maximizing the value of $\delta_{\min}(\mathbf{x}_i, \mathbf{x}_j)$ in (60) as

$$\theta = \begin{cases} \frac{\pi}{2}, \text{BPSK} \\ \frac{\pi}{4}, \text{QPSK} \\ \frac{\pi}{7} \text{or} \left(\frac{\pi}{2} - \frac{\pi}{7}\right), \text{16QAM} \\ \frac{\pi}{16} \text{or} \left(\frac{\pi}{2} - \frac{\pi}{16}\right), \text{64QAM} \end{cases}. \quad (61)$$

VI. Simulation Results

In this section, the performances of the proposed E-GSM, HM-GSM and E-HT-GSM schemes are presented and compared under different antenna configurations. In all the simulation results, perfect channel state information is assumed and the values of the specific θ are selected based on Eq. (59). ML detectors are employed at the receiver for Figs. 8-14. Moreover, the analytical ABEP performances of the proposed systems are added as benchmarkers, which can be obtained by (19). As seen from Fig. 8-14, the upper bound becomes very tight upon increasing the SNR values, which is helpful for evaluating the BER performances of the proposed systems.

Specifically, Figs. 8-10 compare the performances of both the proposed E-GSM, and of the HM-GSM systems to the C-GSM system using $N_t = 4, N_r = 4, N_u = 2$ at different values of M. Fig. 11 compares the complexity of the proposed E-GSM and HM-GSM systems to that of the C-GSM system for the same setups as in Figs. 8-10. The

This work is licensed under a Creative Commons Attribution 3.0 License. For more information, see http://creativecommons.org/licenses/by/3.0/.

This article has been accepted for publication in a future issue of this journal, but has not been fully edited. Content may change prior to final publication. Citation information: DOI 10.1109/ACCESS.2018.2859794, IEEE Access

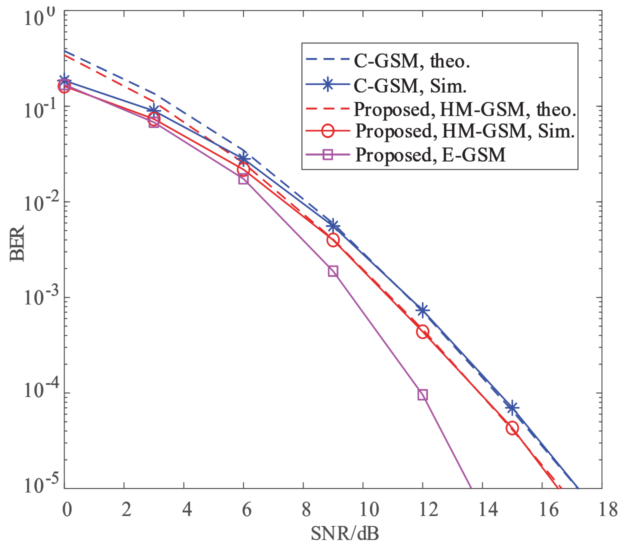

Fig. 9. Performance comparison of the proposed schemes and of the conventional GSM systems using $N_t = 4, N_r = 4, N_u = 2$ and $M = 2$ at 3 bits/symbol.

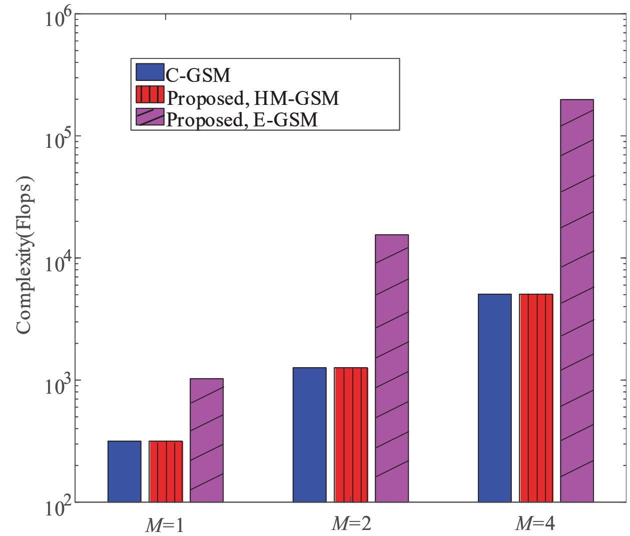

Fig. 11. Complexity comparison of the proposed schemes and of the conventional GSM system using $N_t = 4, N_r = 4$ and $N_u = 2$.

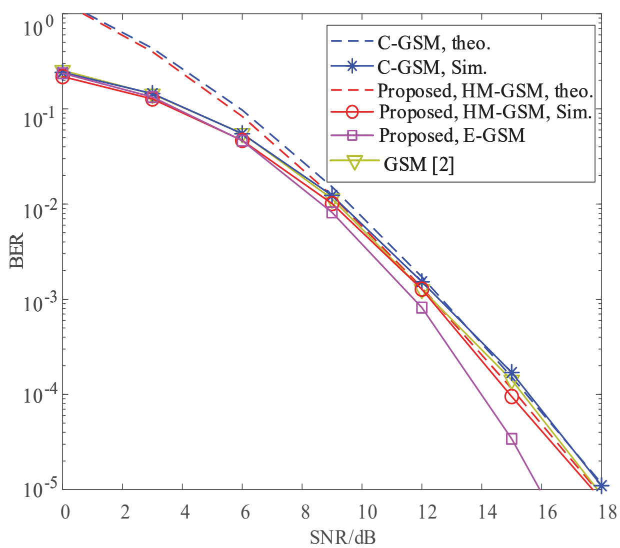

Fig. 10. Performance comparison of the proposed schemes and of the conventional GSM systems using $N_t = 4, N_r = 4, N_u = 2$ and $M = 4$ at 4 bits/symbol.

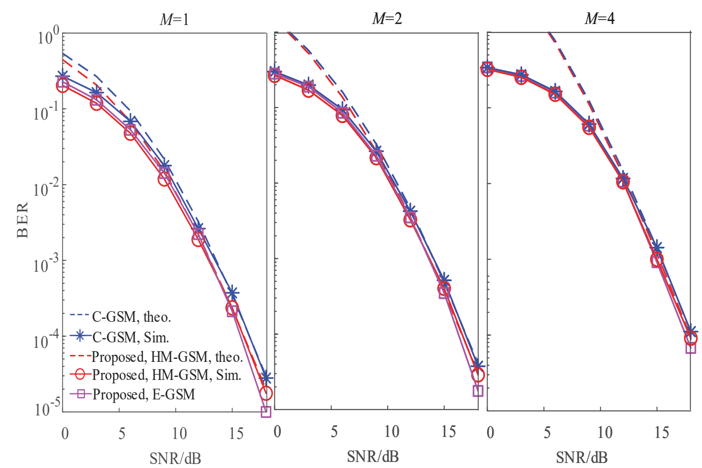

Fig. 12. Performance comparison of the proposed schemes and of the conventional GSM systems using $N_t = 5, N_r = 4, N_u = 3$.

mapping principles of the HM-GSM and C-GSM system are shown in Table VI. Observe from Figs. 8-11 that the proposed E-GSM system is capable of outperforming the C-GSM system by 5 dB, 3.5 dB and 2.5 dB for $M = 1$, $M = 2$ and $M = 4$ respectively at the BER=10^{-5} at an acceptable extra complexity. The proposed HM-GSM scheme is capable of outperforming C-GSM system by 1 dB, 0.6 dB and 0.4 dB for $M = 1$, $M = 2$ and $M = 4$ at the BER=10^{-5} at the same complexity. Moreover, observe from Fig. 10 that the proposed E-GSM and HM-GSM systems also perform better than the scheme in [2].

In order to provide further insights, Figs. 12-13 compare the performances of the proposed E-GSM, HM-GSM to the C-GSM system using $N_t = 5, N_r = 4, N_u = 3$ and $N_t = 6, N_r = 4, N_u = 2$, respectively. Observe from Fig. 12 that the performance advantage of the E-GSM over the C-GSM system becomes modest. This is because for the case of $N_t = 5, N_u = 3$, we have $N_{\text{left}} = 2$, while $N_{\text{same}}/2 = 3$ for $\beta = 2$, $N_{\text{same}}/2 = 1$ for $\beta = 1$, $N_{\text{same}}/2 = 1$ for $\beta = 0$ remain valid according to (12). When the number of common minimum values in $\mathbf{W}$ satisfies $N_{\text{same}}/2 > N_{\text{left}} = 2$, the performance of the optimal TAC set is the same as that of the conventional TAC set. For the case of $N_t = 6, N_r = 4, N_u = 2, N_{\text{left}} = 7$, $N_{\text{same}}/2 = 4$ for $\beta = 1$ and $N_{\text{same}}/2 = 1$ for $\beta = 0$. As a result, $N_{\text{same}}/2 < N_{\text{left}}$ always remains true and the proposed E-GSM system using $N_t = 6, N_r = 4, N_u = 2$ is capable of providing significant performance gain over the C-GSM system, as observed in Fig. 13.

Finally, Fig. 14 compares the performance of the proposed E-HT-GSM system to that of the C-GSM system at different transmission rates. Specifically, for the C-GSM system, we employ QPSK modulation for the cases of $N_t = 4, N_r = 4, N_u = 2$ and $N_t = 8, N_r = 8, N_u = 3$ to obtain the normalized throughput of 6 bits/symbol

This work is licensed under a Creative Commons Attribution 3.0 License. For more information, see http://creativecommons.org/licenses/by/3.0/.

This article has been accepted for publication in a future issue of this journal, but has not been fully edited. Content may change prior to final publication. Citation information: DOI 10.1109/ACCESS.2018.2859794, IEEE Access

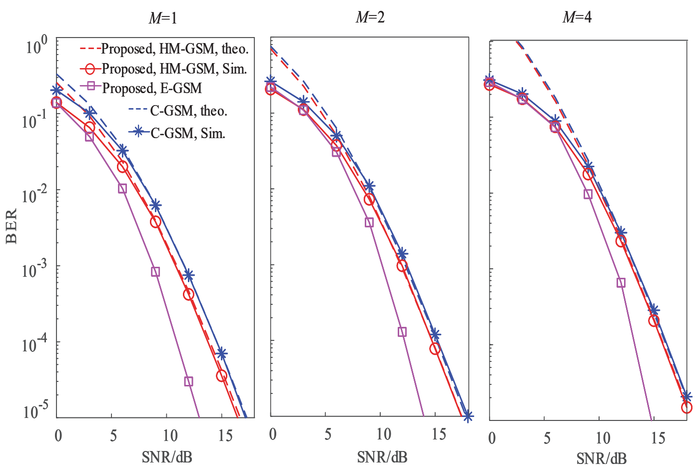

Fig. 13. Performance comparison of the proposed schemes and of the conventional GSM systems using $N_t = 6, N_r = 4, N_u = 2$.

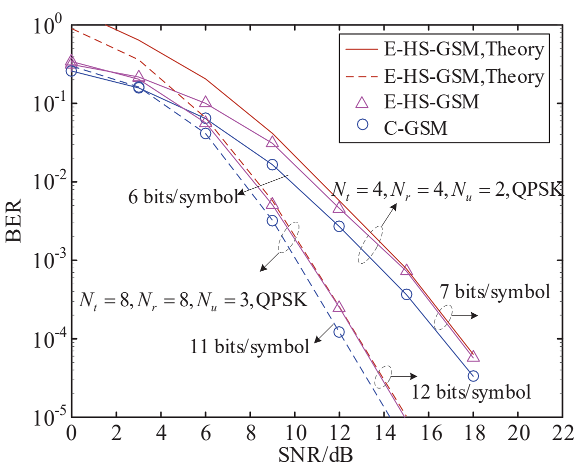

Fig. 14. Performance comparisons of the QPSK-aided E-HT-GSM systems and of the QPSK-aided C-GSM systems using $N_t = 4, N_r = 4, N_u = 2$ and $N_t = 8, N_r = 8, N_u = 3$.

and 11 bits/symbol. For the proposed E-HT-GSM systems relying on the above setups, we achieve an extra bit of throughput, yielding 7 bits/symbol and 12 bits/symbol, respectively. Observe from Fig. 14 that the proposed E-HT-GSM system is capable of increasing the throughput by one bit per channel use at a 0.5 dB performance loss at BER$= 10^{-4}$ for both the above mentioned setups.

VII. Conclusions

The problem of TAC set optimization has been investigated. Firstly, a low-complexity TAC selection algorithm relying on CSI knowledge was designed for our E-GSM systems. Then, hybrid bit-to-TAC mapping based TAC optimization operating without CSI knowledge was designed for the GSM system. The proposed E-GSM system and HM-GSM system are capable of outperforming the C-GSM system at a negligible extra complexity, while the proposed E-HT-GSM system conceived is capable of increasing the throughput per time slot by one bit at a negligible performance loss.

References

[1] A. Younis, N. Serafimovski, R. Mesleh, and H. Haas, "Generalised spatial modulation," *in Proc. 2010 Signals, Syt. Comput.*, Pacific Grove, Nov. 2010, pp. 1498-1502.

[2] J. Wang, S. Jia, and J. Song, "Generalised spatial modulation with multiple active transmit antennas and low complexity detection scheme," *IEEE Trans. Wireless Commun.*, vol. 11, no. 4, pp. 1605-1615, Apr. 2012.

[3] R. Mesleh, H. Haas, S. Sinanovic, C. W. Ahn, and S. Yun, "Spatial modulation," *IEEE Trans. Veh. Technol.*, vol. 57, no. 4, pp. 2228-2241, Jul. 2008.

[4] I. A. Hemadeh, M. E. Hajjar, S. Won, and L. Hanzo, "Layered multi-group steered space-time shift-keying for millimeter-wave communications," *IEEE Access*, Doi:10.1109/ACCESS.2016.2552075, pp. 3708-3718, Apr. 2016

[5] M. Di Renzo, H. Haas, A. Ghrayeb, S. Sugiura, and L. Hanzo, "Spatial modulation for generalized MIMO: challenges, opportunities and implementation," *Proceedings of the IEEE*, vol. 102, no. 1, pp. 56-103, Jan. 2014.

[6] A. Adjoudani, E. C. Beck, A. P. Burg, G. M. Djuknic, t. G. Gvoth, D. Haessig, S. Manji, M. A. Milbrodt, M. Rupp, D. Samardzija, A. B. Siegel, T. Sizer, C. Tran, S. Walker, S. A. Wilkus, P. W. Wolniansky, "Prototype experience for MIMO BLAST over third-generation wireless system," in *IEEE Journal on Selected Areas in Communications*, vol. 21, no. 3, pp. 440-451, 2003.

[7] S. Wang, Y. Li, M. Zhao, and J. Wang, "Energy efficient and low-complexity uplink transceiver for massive spatial modulation MIMO," *IEEE Trans. Veh. Technol.*, vol. 64, no. 10, pp. 4617-4632, Oct. 2015.

[8] S. Wang, Y. Li, and J. Wang, "Multiuser detection in massive spatial modulation MIMO with low-resolution ADCs," *IEEE Trans. Wireless Commun.*, vol. 14, no. 4, pp. 2156-2168, Apr. 2015.

[9] P. Yang, Y. Xiao, Y. Guan, K. V. S. Hari, A. Chockalingam, S. Sugiura, H. Haas, M. D. Renzo, C. Masouros, Z. Liu, L. Xiao, S. Li, and L. Hanzo, "Single-carrier spatial modulation: A promising design for large-scale broadband antenna systems," *IEEE Commun. Surveys Tuts.*, vol. 18, no. 3, pp. 1687-1716, 2016.

[10] T. L. Narasimhan, P. Raviteja and A. Chockalingam, "Generalized spatial modulation in large-scale multiuser MIMO systems," *IEEE Trans. Wireless Commun.* vol. 14, no. 7, pp. 1536-1276, March 2015.

[11] M. Xiao, S. Mumtaz, Y. Huang, L. Dai, Y. Li, M. Matthaiou, G. K. Karagiannidis, E. Bjornson, K. Yang, C. Lin and A. Ghosh, "Millimeter Wave Communications for Future Mobile Networks," *IEEE Journal on Selected Areas in Communications*, vol. 35, no. 9, pp. 1909-1935, 2017.

[12] Y. Xiao, Z. Yang, L. Dan, P. Yang, L. Yin, and W. Xiang, "Low-complexity signal detection for generalized spatial modulation," *IEEE Commun. Lett.*, vol. 18, no. 3, pp. 403-406, Mar. 2014.

[13] C. Yu, S. Hsieh, H. Liang, and C. Lu, "Compressed sensing detector design for space shift keying in MIMO systems," *IEEE Commun. Lett.*, vol. 16, no. 10, pp. 1556-1559, Oct. 2012.

[14] W. Liu, N. Wang, M. Jin, and H. Xu, "Denoising detection for the generalized spatial modulation system using sparse property," *IEEE Commun. Lett.*, vol. 18, no. 1, pp. 22-25, Jan. 2014.

[15] A. G. Rodriguez and C. Masouros, "Low-complexity compressive sensing detection for spatial modulation in large-scale multiple access channels," *IEEE Trans. Commun.*, vol. 63, no. 7, pp. 2565-2579, July 2015.

[16] L. Xiao, P. Yang, Y. Xiao, S. Fan, M. D. Renzo, W. Xiang, and S. Li "Efficient compressed sensing detectors for generalized spatial modulation systems," IEEE Trans. Veh. Technol., vol. pp, no. 99, pp. 1-14, April, 2016.

[17] L. Xiao, P. Yang, Y. Xiao, J. Liu, S. Fan, B. Dong, and S. Li, "An improved soft-input soft-output detector for generalized spatial modulation," *IEEE Signal Proc. Lett.*, vol. 23, no. 1, pp. 30-34, Jan. 2016.

[18] L. Xiao, L. Dan, Y. Zhang, Y. Xiao, P. Yang, and S. Li, "A low-complexity detection scheme for generalized spatial modulation aided single carrier systems," *IEEE Commun. Lett.*, vol. 19, no. 6, pp. 1069-1072, June, 2015.

This work is licensed under a Creative Commons Attribution 3.0 License. For more information, see http://creativecommons.org/licenses/by/3.0/.

This article has been accepted for publication in a future issue of this journal, but has not been fully edited. Content may change prior to final publication. Citation information: DOI 10.1109/ACCESS.2018.2859794, IEEE Access

[19] L. Xiao, P. Yang, Y. Zhao, Y. Xiao, J. Liu, and S. Li,“Low-complexity tree search-based detection algorithms for generalized spatial modulation aided single carrier systems,” in *Proc. IEEE 2016 ICC.*, Malaysia, May, 2016.

[20] T. L. Narasimhan and A. Chockalingam, “On the capacity and performance of generalized spatial modulation”*IEEE Commun. Lett.*, vol. 20, no. 2, pp. 252-255, Nov., 2015.

[21] A. I. Ibrahim, T. Kim and D. J. Love,‘On the achievable rate of generalized spatial modulation using multiplexing under a Gaussian mixture model,” *IEEE Trans. commun.*, vol. 64, no. 4, pp. 1588-1599, Jan., 2016.

[22] K. Takeuchi“Second-order optimality of generalized spatial modulation for MIMO channels with no CSI,”*IEEE wireless Commun. Lett.*, vol. 4, no. 6, pp. 613-616, Sep., 2015.

[23] N. Ishikawa, R. Rajashekar, S. Sugiura and L. Hanzo“Generalized spatial modulation based reduced-RF-chain millimeter-wave communications,” *IEEE Trans. Veh. Technol.*, vol. 66, no. 1, pp. 879-883, 2017.

[24] R. Mesleh, S. S. Ikki, and H. M. Aggoune, “Quadrature spatial modulation,” *IEEE Trans. Veh. Technol.*, vol. 64, no. 6, pp. 2738-2742, June. 2015.

[25] J. Li, M. Wen, X. Cheng, Y. Yan, S. Song, and M. H. Lee, “Generalised pre-coding aided quadrature spatial modulation,” *IEEE Trans. on Veh. Tech.*, vol. 66, no. 2, pp. 1881-1886, 2017.

[26] L. Xiao, P. Yang, S. Fan, S. Li, L. Song, and Y. Xiao, “Low-complexity signal detection for large-scale quadrature spatial modulation systems,”*IEEE Comun. Lett.*, vol. 20, no. 11, pp. 2173-2176, Aug., 2016.

[27] P. Yang, Y. Xiao, B. Zhang, S. Q. Li, M. El-Hajjar, and L. Hanzo, “Star-QAM signaling constellations for spatial modulation,” *IEEE Trans. Veh. Technol.*, vol. 63, no. 8, pp. 3741-3749, Oct. 2014.

[28] P. Yang, Y. Xiao, L. Yin, Q. Tang, S. Q. Li, and L. Hanzo, “Hybrid bit-to-symbol mapping for spatial modulation,” *IEEE Trans. Veh. Technol.*, vol. 65, no. 7, pp. 5804-5810, July. 2015.

[29] M. Maleki, H. Reza Bahrami, A. Alizadeh, and N. H. Tran, “On the performance of spatial modulation: optimal constellation breakdown,”*IEEE Trans. Commnun.*, vol. 62, no. 1, pp. 144-157, Jan. 2014.

[30] C.-C. Cheng, H. Sari, S. Sezginer and Y. T. Su, “Enhanced spatial modulation with multiple signal constellations,”*IEEE Trans. Commun.*, vol. 63, no. 6, June 2015, pp. 2237-48.

[31] O. Osman, “Variable active antenna spatial modulation,”*IEEE IET Microwaves, Antennas Propagation* vol. 9, no. 15, pp. 1816-1824 Oct. 2015.

[32] P. Koundinya, K. V. S. Hari, and L. Hanzo, “Joint design of the spatial and of the classic symbol alphabet improves single-RF spatial modulation,”*IEEE Access*, vol. 4, pp. 10246-10257. Aug. 2016.

[33] P. Yang, Y. Xiao, Y. Yu, abd S. Q. Li, “Adaptive spatial modulation for wireless MIMO transmission systems,” *IEEE Commun. Lett.*, vol. 15, no. 6, pp. 602-606, Jun. 2011.

[34] P. Yang, Y. Xiao, L. Li, Q. Tang, and S. Q. Li, “Link adaptation for spatial modulation with limited feedback,” *IEEE Trans. Veh. Technol.*, vol. 61, no. 8, pp. 3808-3813, Oct. 2012.

[35] R. Rajashekar, K. V. S. Hari, and L. Hanzo, “Antenna selection in spatial modulation systems,” *IEEE Commun. Lett.*, vol. 17, no. 3, pp. 521-524, Mar. 2013.

[36] N. Pillay and H. Xu, “Comments on ‘Antenna selection in spatial modulation systems’,” *IEEE Commun. Lett.*, vol. 17, no. 9, pp. 1681-1683, Sep. 2013.

[37] S. Jin, W. Choi, J. Park, and D. Park, “Linear precoding design for mutual information maximization in generalized spatial modulation with finite alphabet inputs,”*IEEE Commun. Lett.*, vol. 19, no. 8, pp. 1323-1327, Aug., 2015.

[38] X. Li, N. Zhao, Y. S, F. R. Yu, “ Interference alignment based on antenna selection with imperfect channel state information in Cingnitive radio networks,”. *IEEE Trans. Veh. Technol.*, vol. 65, no. 7, pp. 5497-5511, June 2015.

[39] N. Zhao, F. R. Yu, H. Sun, A. Nallanathan, H. Yin, “A novel interference alignment scheme based on sequential antenna switching in wireless networks.” *IEEE Trans. Wireless Coummn.*, vol. 12, no. 10, pp. 5008-5021, Sep. 2013.

[40] P. Yang, Y. Guan, Y. Xiao, M. Renzo, S. Li and L. Hanzo, “Transmit precoded spatial modulation: Maximizing the minimum euclidean distance verus minimizing the bit error ratio” *IEEE Trans. wireless Commun.*, vol. 15, no. 3, pp. 2054-2068, March 2016.

[41] J. Jeganathan, A. Ghrayeb, and L. Szczecinski, “Generalized space shift keying modulation for MIMO channels,” in *Proc. IEEE Int. Symp. Personal, Indoor, Mobile Radio Commun.*, Cannes, Sep. 2008, pp. 1-5.

[42] E. Basar, U. Aygolu, E. Panayirci and H. V. Poor, “Space-Time Block Coded Spatial Modulation,” *IEEE Trans. Commun.*, vol. 59, no. 3, pp. 823-832, Mar. 2011.

Lixia Xiao received the B.E., M.E., and Ph. D degrees in 2010, 2013 and 2017, respectively from University of Electronic Science and Technology of China (UESTC). Currently, she is a research fellow with the department of Electrical Electronic Engineering of University of Surrey. Her research is in the field of wireless communications and communication theory. In particular, she is very interested in signal detection and performance analysis of wireless communication systems.

Pei Xiao (SM’11) is a professor of Wireless Communications at the Institute for Communication Systems, home of 5G Innovation Centre (5GIC) at the University of Surrey. He is the technical manager of 5GIC, leading the research team at on the new physical layer work area, and coordinating/supervising research activities across all the work areas within 5GIC (www.surrey.ac.uk/5gic research). Prior to this, he worked at Newcastle University and QueenâĂŹs University Belfast. He also held positions at Nokia Networks in Finland. He has published extensively in the fields of communication theory and signal processing for wireless communications.

Yue Xiao (M’04’) received the Ph.D degree in communication and information systems from the University of Electronic Science and Technology of China (UESTC) in 2007. He is currently a Professor with National Key Laboratory of Science and Technology on Communications, UESTC. He has published more than 100 international journals and has been in charge of more than 20 projects in the area of Chinese 3G/4G/5G wireless communication systems. He is an inventor of more than 50 Chinese and PCT patents on wireless systems. His research interests are in system design and signal processing toward future wireless communication systems. He currently serves as an Associate Editor of IEEE COMMUNICATIONS LETTERS.

Chaowu Wu received the bachelor degree in 2016 from University of Electronic Science and Technology of China (UESTC). Currently, he is working towards the master degree in National Key Laboratory of Science and Technology on Communications in UESTC. His main research work is focus on precoding, signal detection and performance analysis of wireless communications.

This work is licensed under a Creative Commons Attribution 3.0 License. For more information, see http://creativecommons.org/licenses/by/3.0/.

This article has been accepted for publication in a future issue of this journal, but has not been fully edited. Content may change prior to final publication. Citation information: DOI 10.1109/ACCESS.2018.2859794, IEEE Access

Ibrahim A. Hemadeh received his B.Eng. degree (with first class honours) in Computer and Communications Engineering from the Islamic University of Lebanon, Lebanon, in 2010. He then received his M.Sc. degree in Wireless Communications (with distinction) and his Ph.D. degree in Electronics and Electrical Engineering from the University of Southampton, UK, in 2012 and 2017, respectively. He is currently a postdoctocal researcher at Southampton Wireless (SW) group, University of Southampton, UK. His research interests mainly include millimeter-wave communications, multi-functional MIMO, multi-dimensional (time-space-and frequency) transceiver designs, channel coding as well as multi-user MIMO.

Lajos Hanzo (http://www-mobile.ecs.soton.ac.uk) FREng, FIEEE, FIET, Fellow of EURASIP, DSc received his degree in electronics in 1976 and his doctorate in 1983. In 2009 he was awarded the honorary doctorate "Doctor Honoris Causa" by the Technical University of Budapest and in 2015 by the UNiversity of Edinburgh. During his 40-year career in telecommunications he has held various research and academic posts in Hungary, Germany and the UK. Since 1986 he has been with the School of Electronics and Computer Science, University of Southampton, UK, where he holds the chair in telecommunications. He has successfully supervised 112 PhD students, co-authored 18 John Wiley/IEEE Press books on mobile radio communications totalling in excess of 10 000 pages, published 1759 research contributions at IEEE Xplore, acted both as TPC and General Chair of IEEE conferences, presented keynote lectures and has been awarded a number of distinctions. Currently he is directing a 40-strong academic research team, working on a range of research projects in the field of wireless multimedia communications sponsored by industry, the Engineering and Physical Sciences Research Council (EPSRC) UK, the European Research Council's Advanced Fellow Grant and the Royal Society's Wolfson Research Merit Award. He is an enthusiastic supporter of industrial and academic liaison and he offers a range of industrial courses. He is also a Governor of the IEEE VTS. During 2008-2012 he was the Editor-in-Chief of the IEEE Press and a Chaired Professor also at Tsinghua University, Beijing. His research is funded by the European Research Council's Advanced Research Fellow Grant. For further information on research in progress and associated publications please refer to http://www-mobile.ecs.soton.ac.uk

Hung Viet Nguyen (S'09-M'14) received the B.Eng. degree in Electronics & Telecommunications from Hanoi University of Science and Technology (HUST), Hanoi, Vietnam, in 1999 and his M.Eng. in Telecommunications from Asian Institute of Technology (AIT), Bangkok, Thailand, in 2002. Since 1999 he has been a lecturer at the Post & Telecommunications Institute of Technology (PTIT), Vietnam. He worked for the OPTIMIX and CONCERTO European as well as EPSRC funded projects. He is currently a research fellow at 5G Innovation Centre, University of Surrey, UK. His research interests include cooperative communications, channel coding, network coding and quantum communications.

This work is licensed under a Creative Commons Attribution 3.0 License. For more information, see http://creativecommons.org/licenses/by/3.0/.